Natural Resources Canada / Ressources naturelles Canada

GEOLOGICAL SURVEY OF CANADA
PREPRINT 3

# Geophysical contributions to a synthesis of western Churchill geology and metallogeny

V. Tschirhart, S. Pehrsson, N. Wodicka, J.A. Percival,
C.W. Jefferson, T. Peterson, and R.G. Berman

2022

Canada

GEOLOGICAL SURVEY OF CANADA
PREPRINT 3

# Geophysical contributions to a synthesis of western Churchill geology and metallogeny

**V. Tschirhart[1*], S. Pehrsson[1], N. Wodicka[1], J.A. Percival[1], C.W. Jefferson[1], T. Peterson[1], and R.G. Berman[1]**

[1]Geological Survey of Canada, 601 Booth Street, Ottawa, Ontario
*Corresponding author: victoria.tschirhart@nrcan-rncan.gc.ca

## 2022



Permanent link: https://doi.org/10.4095/330639
ISBN 978-0-660-45403-0
Catalogue No. M183-7/3-2022E-PDF

This publication is available for free download through GEOSCAN (https://geoscan.nrcan.gc.ca/).

**Recommended citation**
Tschirhart, V., Pehrsson, S., Wodicka, N., Percival J.A., Jefferson, C.W., Peterson, T., and Berman, R.G., 2022. Geophysical contributions to a synthesis of western Churchill geology and metallogeny; Geological Survey of Canada, Preprint 3, 47 p. https://doi.org/10.4095/330639



The final version of this manuscript will be released in the following volume: Pehrsson, S., Wodicka, N., Rogers, N., and Percival, J.A., (ed.), in press. Canada's northern shield: new perspectives from the Geo-mapping for Energy and Minerals program; Geological Survey of Canada, Bulletin 612.

## Abstract

The geophysical data sets available for the western Churchill Province have had a bearing on the understanding of its structure, evolution and metal endowment. New data were acquired and interpreted during the Geo-mapping for Energy and Minerals (GEM) Program (2008–2020). Regional, high-resolution aeromagnetic, and targeted gravity and magnetotelluric surveys were collected in GEM, in conjunction with geological mapping projects, in order to provide control on bedrock features beneath widespread glacial overburden and flat-lying sedimentary basins. Quantitative estimates of three-dimensional geometry were obtained in key areas through geophysical models integrating the geophysical characteristics with local rock property measurements. These geophysical data sets contributed to new knowledge and interpretations in three related research fields: 1) location and nature of Rae craton's boundaries within the western Churchill Province; 2) definition of internal Rae architecture; and 3) identification of reactivated structures controlling gold and uranium mineralization. The new data, models and emerging tectonic and metallogenic frameworks will serve as guides for future exploration in this remote, complex, challenging region.

## Résumé

Les ensembles de données géophysiques disponibles pour la partie occidentale de la Province de Churchill ont eu une influence sur la compréhension de sa structure, de son évolution et de sa richesse en métaux. Le Programme de géocartographie de l'énergie et des minéraux (GEM) [2008-2020] a permis l'acquisition et l'interprétation de nouvelles données. Des levés aéromagnétiques régionaux à haute résolution, ainsi que des levés gravimétriques et magnétotelluriques ciblés, ont été réalisés dans le cadre du Programme de GEM, parallèlement à des projets de cartographie géologique. Les données recueillies nous permettent d'assurer le suivi des entités du substratum rocheux se trouvant sous la vaste couverture de débris glaciaires et les bassins sédimentaires horizontaux. Nous avons obtenu des estimations quantitatives de la géométrie tridimensionnelle dans des zones clés grâce à des modèles géophysiques intégrant les caractéristiques géophysiques et les mesures des propriétés des roches de la région. Ces ensembles de données géophysiques ont contribué à l'actualisation des connaissances et des interprétations dans trois domaines de recherche connexes : 1) l'emplacement et la nature des limites du craton de Rae dans la partie occidentale de la Province de Churchill; 2) la définition de l'architecture interne de Rae; 3) la détermination des structures réactivées contrôlant les minéralisations aurifères et uranifères. Les nouvelles données, les modèles et les cadres tectoniques et métallogéniques émergents permettront d'orienter l'exploration future de cette région éloignée, complexe et pleine de défis.

## 1. INTRODUCTION

Regional, publically available gravity and magnetic datasets are widely used in mineral exploration and geological mapping programs throughout the world. Lateral changes in the physical properties mapped by these methods—magnetic susceptibility and density—may be the result of different lithological, structural, metamorphic, or mineralogical characteristics, or reflect the cumulative deformation and alteration history of the crust. By incorporating additional parameters such as bedrock maps, rock physical properties, geochronological and geochemical datasets, the geophysical interpretations can be linked to ground observations. As such, regional geophysical datasets are valuable in remote locations where field costs are high, glacial overburden may be extensive, and detailed ground-truthing may not be possible. Fortunately, key reference localities can be established to calibrate geophysical responses with geological observations in order to extrapolate interpretations over broad areas. Airborne geophysical surveys are a particularly cost-effective means of covering vast tracts of land with systematic data sets. Furthermore, where used with multiple geoscience observations, regional geophysical datasets help answer fundamental questions about the tectonic framework, lithology, and three-dimensional (3D) structure of the crust (*e.g.* Cook *et al.*, 2012).



Prior to initiation of the Geo-mapping for Energy and Minerals (GEM) Program, many parts of the northern Canadian Shield, in particular the western Churchill Province, comprising the Rae and Hearne cratons and Chesterfield block (Figure 1), were underexplored as a result of inaccessibility and coarse geoscience information. Existing potential field datasets included regional ground gravity stations that resolved features >25 km, and sparse high-resolution gravity transects. Aeromagnetic coverage acquired prior to 1980 comprised predominantly 805 m-spaced (1/2 mile) lines. Such low-resolution data made all but the most rudimentary interpretations tenuous. Bedrock in northern Canada is largely obscured by glacial overburden, making aeromagnetic maps an essential tool for geological mapping and mineral exploration. To generate new knowledge, assess the resource potential of the landmass, and to support bedrock mapping programs under GEM, the Geological Survey of Canada (GSC) has been updating, infilling, and modernizing geophysical datasets over key regions (Figure 2). This initiative included the acquisition of 24 airborne geophysical surveys (Table 1) over the areas included in this synthesis volume, a series of ground gravity surveys across key geological transects (Thomas, 2012; Tschirhart *et al.*, 2013a; 2013b; 2013d; 2015; 2016; 2017), and several magnetotelluric surveys (Spratt *et al.*, 2011, 2012a, 2013a, 2013b; 2014; Roberts *et al.*, 2015).  For interpretations and surveys on parts of the western Churchill province not discussed herein (*i.e.* on Baffin Island), the reader is directed to the references in Table 1.

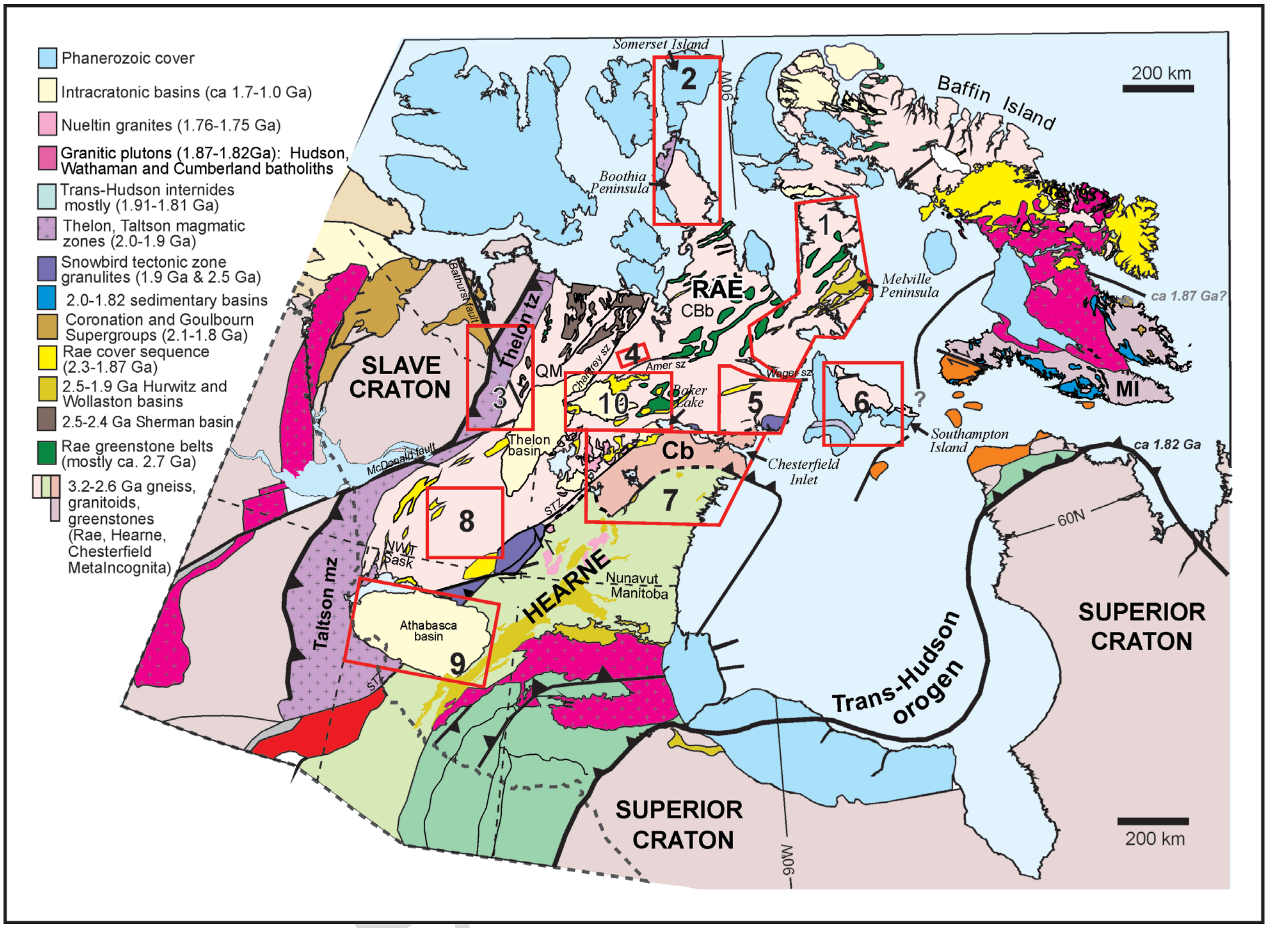


**Figure 1:** Simplified geological map of the western Churchill Province and surrounding crustal blocks from Berman et al. (2005). Areas discussed in text shown by red boxes: 1 = Melville Peninsula; 2 = Boothia Peninsula and Somerset Island; 3 = Thelon tectonic zone; 4 = Montresor Belt; 5 = Tehery Lake and Wager Bay; 6 = Southampton Island; 7 = Chesterfield Inlet; 8 = South Rae; 9 = Athabasca Basin; 10 = Thelon Basin. Abbreviations: Amer sz = Amer shear zone; Chantrey sz = Chantrey shear zone; Cb = Chesterfield block; CBb = Committee Bay block; MI = Meta Incognita microcontinent; QM = Queen Maud block; STZ = Snowbird Tectonic Zone; Thelon tz = Thelon tectonic zone; Taltson mz = Taltson magmatic zone; Wager sz = Wager shear zone. Note geology southwest of dashed line is covered by the Phanerozoic Western Canada Sedimentary Basin.

This contribution summarizes select integrated interpretations, potential-field geophysical innovations, and modelling products generated for parts of the Rae craton, Hearne craton, and

Chesterfield block under the GEM I and II Programs. We first introduce the key areas of interest and provide an overview of the geophysical activities in these regions completed under GEM. This is followed by a discussion of the regional implications. By comparing distinct, but comprehensive integrated interpretations, we highlight regional-scale linkages to better understand the 3D crustal structure and mineral endowment of this remote region.

## 2. REGIONAL GEOLOGICAL SETTING

The Canadian Shield region north of 60° encompasses the 3.5–2.5 Ga Rae and 3.0–2.65 Ga Hearne cratons, comprising the western Churchill province, the 4.0–2.5 Ga Slave craton, parts of the northern Superior craton, and younger Paleoproterozoic orogens that welded them (Hoffman, 1988; Wheeler *et al.*, 1996; Figure 1). We herein summarize our prime interest, the Rae craton; for summaries of the Hearne and Slave craton geology, the reader is referred respectively to Davis *et al.* (2004), Hanmer *et al.* (2004) and Helmstaedt and Pehrsson (2012). A summary of post-1.6 Ga mafic magmatic events in the northern Canadian Shield can be found in Buchan and Ernst (this volume).

The Rae craton, within which we include the Chesterfield block (Berman *et al.*, 2007), underlies most of the study region and extends from beneath Phanerozoic cover in Saskatchewan and Alberta through mainland Nunavut, Northwest Territories, and central Baffin Island (Figure 1; Berman *et al.*, 2005). It predominantly comprises Meso- to Neoarchean plutonic and volcano-sedimentary rocks including a widespread magmatic suite, the 2.62–2.58 Ga Snow Island Suite (Peterson *et al.*, 2015a; this volume). The subsequent reworking of the Rae craton is complex (Berman, 2010), involving five major tectonometamorphic events: the 2.56–2.52 Ga MacQuoid orogeny which affected the Committee Bay and Chesterfield blocks (Davis *et al.,* 2006); the 2.50–2.35 Ga Arrowsmith orogeny which reworked the western Rae margin from Saskatchewan to Baffin Island (Berman *et al.*, 2013a); the 2.0–1.92 Ga Taltson-Thelon orogeny which involved accretion of the Slave and Buffalo Head terranes to the west (Chacko *et al.*, 2000; Ross, 2002; Berman *et al.*, 2016; Whalen *et al.*, 2018); the 1.92–1.88 Ga Snowbird orogeny which accreted the Hearne craton to the east (Berman *et al.*, 2007; Thiessen et al. 2018), and variable effects of the widespread 1.87–1.80 Ga Trans-Hudson orogeny (Pehrsson *et al.*, 2013; Regis et al. 2021). An extensive Paleoproterozoic cover sequence, deposited *ca.* 2.29–1.88 Ga, overlies the crystalline basement (Rainbird *et al.*, 2010). The component Amer, Ketyet River, Montresor, and Chantrey groups formed part of a broad, epicratonic sedimentary system that extended to the Piling and Penrhyn groups of the northeastern Rae craton where an incipient ocean basin may have formed (Wodicka *et al.*, 2014; Percival *et al.*, 2017 and references therein). Owing to effects of the Trans-Hudson orogeny, only remnants of the Rae cover sequence are preserved in elongate northeast-trending, synformal belts.

The Chesterfield block comprises 2.75–2.64 Ga back arc-like supracrustal belts (Sandeman *et al.* 2006; Acosta-Góngora *et al.*, 2018 and references therein) and collided with the Rae craton at or prior to 2.6 Ga (Berman *et al.*, 2007). Its southern boundary may be demarcated by the Tyrrell shear zone, and the *ca.* 1.8 Ga Happy Lake and Panartoq Points shear zones (Pehrsson *et al.*, this volume), which thrust the domain over the Hearne craton. The cryptic *ca.* 1.90 Ga Snowbird Tectonic Zone (STZ) (Berman *et al.*, 2007) bounds the Rae craton to the east, separating Rae craton and Chesterfield block from the Hearne craton, and is excised by the younger Happy Lake and Panartoq structures.

Two major Paleoproterozoic magmatic suites were intruded into the Rae craton at the end of, and following, the Trans-Hudson orogeny. The 1.85–1.80 Ga Hudson granite suite (van Breemen *et al.*, 2005) was emplaced late-syntectonically and has been interpreted as the product of intracrustal melting during thickening (Peterson *et al.*, 2002). The 1.77–1.73 Ga Kivalliq igneous suite, including the Nueltin rapikivi granite, mafic dykes, and bimodal volcanic rocks within the Wharton Group, extend from Somerset Island to southern Saskatchewan (Hayward *et al.*, 2013; Peterson *et al.*, 2015c).

Following Trans-Hudson orogenesis and regional exhumation and cooling (Kellett *et al.*, 2020), older Archean basement and Paleoproterozoic cover of the western Churchill Province were overlain by the Dubawnt (Rainbird *et al.*, 2003) and Athabasca Supergroups (Ramaekers *et al.*, 2007), which occur in intracontinental basins. The Dubawnt Supergroup comprises three unconformity-bounded, largely clastic sequences: the 1840–1785 Ma Baker Lake, 1780–1750 Ma Wharton, and 1700–1500 Ma Barrensland Groups. The Barrensland Group is exposed in Thelon Basin (Figure 1) and includes the Thelon, Kuungmi, and Lookout Point formations. The Dubawnt Supergroup is broadly stratigraphically and tectonically similar to the 1760–1500 Ma Athabasca Supergroup (Ramaekers *et al.*, 2007) of the Athabasca Basin in Saskatchewan, host to the world's highest grade, large tonnage uranium deposits (Figure 1).



## 3. GEOPHYSICAL DATASETS

The interpretation and modelling process was based on multiple geophysical datasets described below. The regional aeromagnetic data were acquired as part of Canada's National Aeromagnetic Surveying program that began in 1947, which included systematic surveys over Canada along 805 m (½ mile) spaced lines acquired at a nominal terrain clearance of ~300 m. These data were gridded to

200 m using minimum curvature (Figure 2). More modern surveys acquired during GEM I and II (Table 1) were, for the most part, flown along 400 m spaced lines (Table 1).

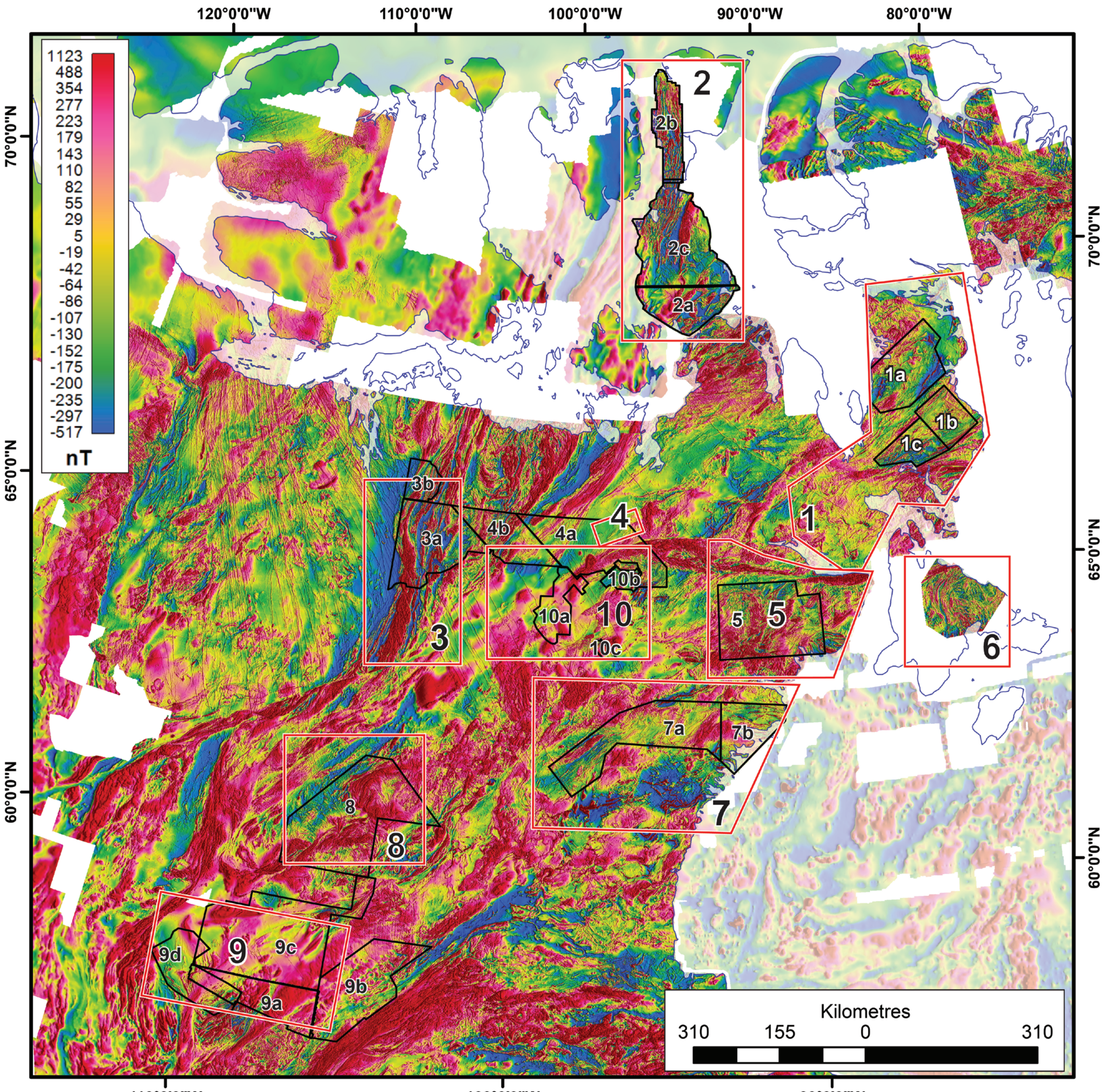


**Figure 2:** Residual total field map. Project areas discussed in text outlined by red boxes and labelled as in Figure 1. Black boxes and white labels show GEM I and GEM II airborne survey locations discussed in the text from Table 1.

**Table 1:** Aeromagnetic surveys in the western Churchill Province flown under GEM.

| Label | Program | Survey Name | Data | Year | Spacing (m) | Project | Publications |
|---|---|---|---|---|---|---|---|
| 1a | GEM I | Sarcpa Lake | Mag | 2009 | 400 | Melville Peninsula | Corrigan et al., 2013; Spratt et al., 2013; LaFlamme et al., 2014 |
| 1b | GEM I | Miertsching Lake East | Mag, Rad | 2009 | 400 | Melville Peninsula | Corrigan et al., 2013; Spratt et al., 2013; LaFlamme et al., 2014 |
| 1c | GEM I | Miertsching Lake West | Mag, Rad | 2009 | 400 | Melville Peninsula | Corrigan et al., 2013; Spratt et al., 2013; LaFlamme et al., 2014 |
| 2a | GEM II | Northern Boothia Peninsula | Mag | 2013 | 400 | Boothia | Sanborn-Barrie et al., 2018 |
| 2b | GEM II | Somerset Island | Mag | 2014 | 400 | Boothia | Sanborn-Barrie et al., 2018 |
| 2c | GEM II | Northern Boothia Peninsula II | Mag | 2016 | 400 | Boothia | Sanborn-Barrie et al., 2018 |
| 3a | GEM II | Duggan Lake I & II | Mag | 2014 | 400 | Chantrey-Thelon | Roberts et al., 2015; Berman et al., 2018; Ma, 2018 |
| 3b | GEM II | Overby-Duggan | Mag | 2017 | 400 | Chantrey-Thelon | Roberts et al., 2015; Berman et al., 2018; Ma, 2018 |
| 4a | GEM II | Garry Lake | Mag | 2012 | 400 | Chantrey-Thelon | Percival et al., 2015; Tschirhart et al., 2015; Percival and Tschirhart, 2017 |
| 4b | GEM II | Pelly Lake | Mag | 2012 | 400 | Chantrey-Thelon | Roberts et al., 2015; Berman et al., 2018; Ma, 2018 |
| 5 | GEM II | Tehery Lake | Mag | 2012 | 400 | Tehery-Wager | Wodicka et al., 2016; Wodicka et al., 2017; Tschirhart et al., 2016 |
| 7a | GEM I | Chesterfield Inlet - block AB | Mag | 2009 | 400 | Chesterfield | Pehrsson et al., 2014 |
| 7b | GEM I | Chesterfield Inlet - block C | Mag | 2009 | 400 | Chesterfield | Pehrsson et al., 2014 |
| 8 | GEM II | NTGO-GSC - South Rae Craton | Mag | 2012 | 400 | South Rae | Percival et al., 2016; Jamison et al., 2017; Martell et al., 2018; Mowbray et al., 2019 |
| 9a | GEM I | Southern Athabasca Basin | Mag, Rad | 2008 | 400 | Athabasca | Card et al., 2010 |
| 9b | GEM I | Eastern Athabasca Basin | Mag, Rad | 2009 | 400 | Athabasca | Card et al., 2010 |
| 9c | GEM I | N.W. Athabasca Basin | Mag, Rad | 2010 | 400 | Athabasca | Card et al., 2010 |
| 9d | TGI-5 | Marguerite River | Mag | 2017 | 400 | Athabasca | Tschirhart et al., submitted; TGI synthesis that talk about U |
| 10a | GEM I | N.E. Thelon Basin area 1-2-3 | Mag, Rad | 2009 | 400 | Northeast Thelon | Calhoun et al., 2014; Hayward et al., 2013; Tschirhart et al., 2011a; 2013a, 2013b, 2013c, 2013d, 2014, 2017; Tschirhart, 2014; Peterson et al., 2015a, 2015b, 2015c, this volume; Jefferson et al., 2015; this volume |
| 10b | GEM I | N.E. Thelon Basin area 6 | Mag, Rad | 2009 | 400 | Northeast Thelon | Calhoun et al., 2014; Hayward et al., 2013; Tschirhart et al., 2011a; 2013a, 2013b, 2013c, 2013d, 2014, 2017; Tschirhart, 2014; Peterson et al., 2015a, 2015b, 2015c, this volume; Jefferson et al., 2015; this volume |
| 10c | GEM I | N.E. Thelon Basin area 5 | Mag, Rad | 2009 | 400 | Northeast Thelon | Calhoun et al., 2014; Hayward et al., 2013; Tschirhart et al., 2011a; 2013a, 2013b, 2013c, 2013d, 2014, 2017; Tschirhart, 2014; Peterson et al., 2015a, 2015b, 2015c, this volume; Jefferson et al., 2015; this volume |
| | GEM I | NTGO-GSC - Minto Inlier | Mag, Rad | 2010 | 400 | Victoria Island | |
| | GEM I | NTGO-GSC - N. Great Bear Magmatic Zone | Mag, Rad | 2009 | 400 | Great Bear | Hayward et al., 2013; Hayward et al., 2014; Enkin et al., 2016; Hayward et al., 2016 |
| | GEM I | Great Island – Seal River | Mag, Rad | 2008 | 400 | Great Island | Anderson et al., 2009; Anderson et al., 2010 |
| | GEM I | Cumberland Peninsula A | Mag | 2008 | 400 | Baffin Island | * |

| | | | | | | | |
|---|---|---|---|---|---|---|---|
| | GEM I | Cumberland Peninsula B | Mag | 2008 | 400 | Baffin Island | * |
| | GEM II | Amittok Lake | Mag | 2015 | 400 | Baffin Island | * |
| | GEM II | McKeand River | Mag | 2015 | 400 | Baffin Island | * |
| *Baffin publications summarized in Baffin Synthesis Volume | | | | | | | |

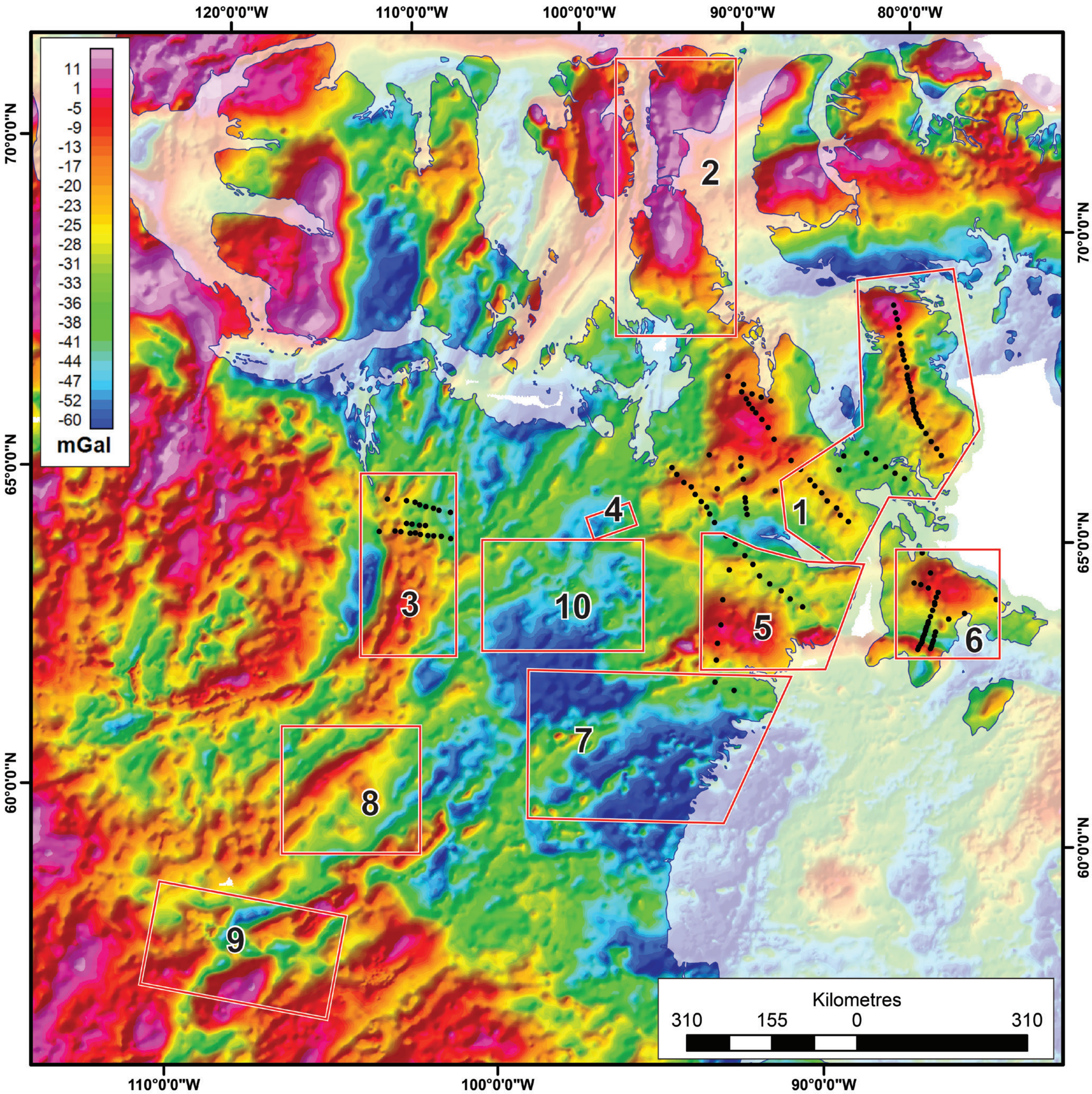


**Figure 3:** Isostatic residual Bouguer gravity map. Project areas discussed in text outlined by red boxes and labelled as in Figure 1. GEM MT stations plotted as black dots.

From 1944 to present, the Earth Physics Branch (now part of the GSC), Surveys and Mapping Branch and the GSC have been acquiring ground gravity stations at an average spacing of 10–15 km. The ground gravity data were corrected for latitude, instrument drift, elevation, and Earth's tides, followed by application of Free Air and Bouguer corrections. The data were reduced to a Bouguer slab density of 2.67 g/cm$^3$ and gridded to 2 km using minimum curvature. The isostatic residual was removed using the methodology defined in Jobin *et al.* (2017) (Figure 3). In addition, during GEM, a number of detailed surveys were conducted and interpreted across key transects (Thomas, 2012; Tschirhart, 2014; Tschirhart *et al.*, 2013a, 2013b, 2013d; 2015; 2017) to provide information on the geometry of shallow crustal features. Individual transects and data reduction are described in the aforementioned publications. Many of the archival gravity stations include density information (available through the Canadian Geoscience Data Repository). Rock properties provide the linkage between geological and geophysical information. To constrain the interpretations and modelling products produced under GEM, additional magnetic susceptibility and density data were acquired (Thomas, 2012; Enkin *et al.*, 2016, Tschirhart, 2014; Tschirhart *et al.*, 2017; Enkin, 2018) on archival and new samples. These data are available through the Canadian Geoscience Data Repository (http://gdr.agg.nrcan.gc.ca/gdrdap/dap/search-eng.php) or in Enkin (2018).

Long period and broadband magnetotelluric (MT) stations were established along several transects within the study area (Figure 3). The acquisition, processing, and preliminary results are outlined in Spratt *et al.* (2011, 2012a, 2012b, 2013a, 2013b) and Roberts *et al.* (2015).

### *3.1 Geophysical-geological interpretation: an example from the northeast Thelon Basin*

Despite the reconnaissance nature of regional potential field datasets, meaningful unique geological solutions can be generated from them. An example of the integration of geological and geophysical information is presented for the northeast Thelon Basin. Stratigraphically and tectonically similar to the Athabasca Basin, the northeast Thelon Basin (Figure 1) is similarly prospective for unconformity-related uranium deposits in and around the Kiggavik camp (Figure 4a) and was the subject of extensive geological and geophysical studies under the GEM Uranium project (see overview by Jefferson *et al.* (this volume)). Following compilation, levelling, and stitching of nine industry surveys (Tschirhart *et al.*, 2011a), three airborne magnetic and radiometric surveys were flown to infill the gaps between the high-resolution industry surveys (Table 1) provided by a collaborative consortium that shared their airborne geophysical data (Jefferson *et al.*, 2011). This resulted in an extensive compilation of high-resolution and/or modern airborne coverage over most of the northeast Thelon Basin (Figures 2, 4a). The new compilation, coupled with bedrock mapping, ground gravity transects, and rock property measurements, formed the backbone of numerous geophysical interpretations in the region. The initial studies (Tschirhart *et al.*, 2013a, 2013b, 2013d) were conducted outside the northeast Thelon Basin margins, with the structural style and geophysical characteristics of the rock packages informing the later interpretations of the sub-Thelon basement (Tschirhart and Pehrsson, 2016; Tschirhart *et al.*, 2014, 2017).

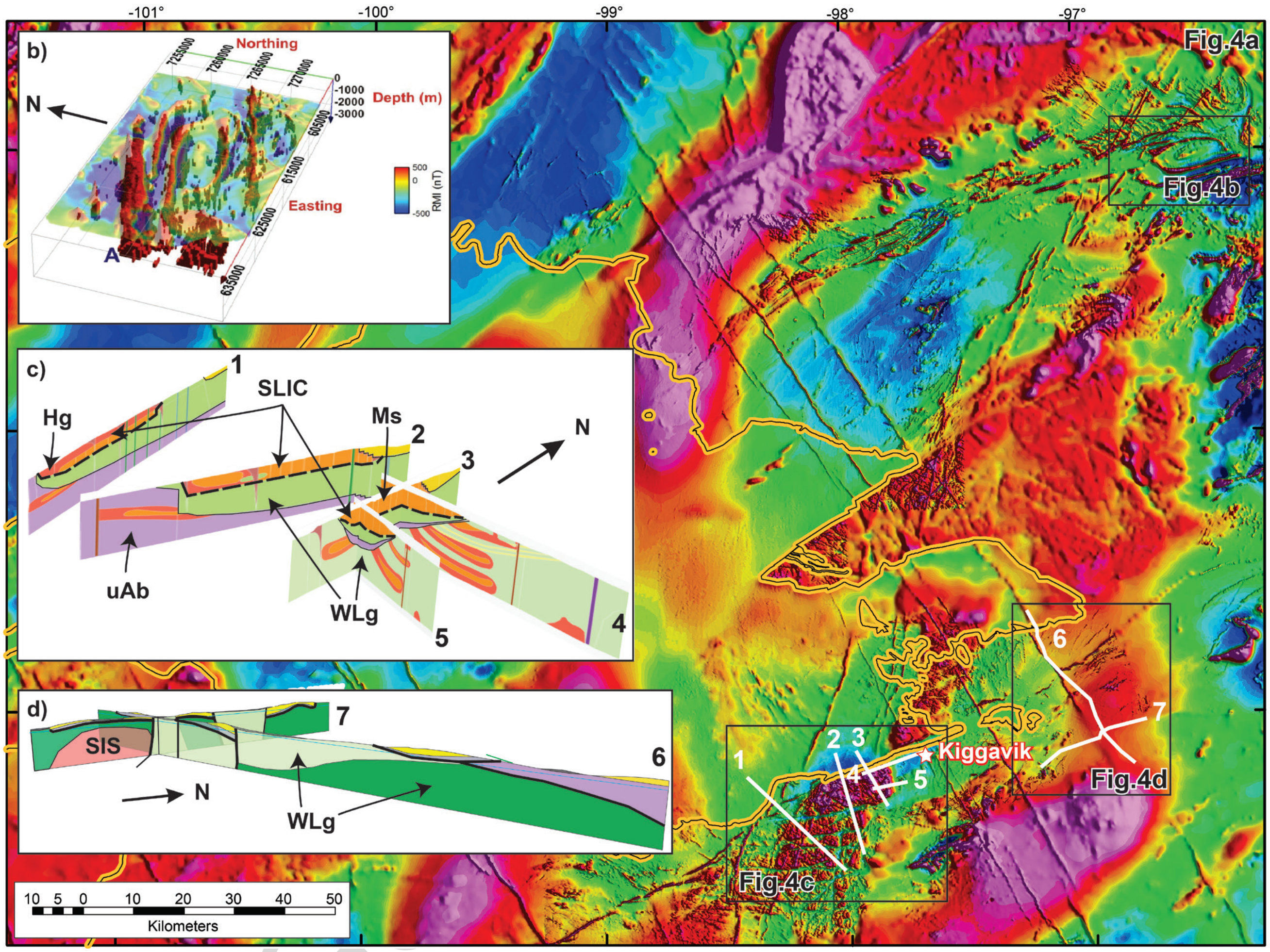


**Figure 4:** a) Merged residual total field map of the northeast Thelon Basin as outlined in beige. Areas discussed in text and visualized in the panels outlined by black boxes; gravity transects denoted by white lines and labelled as in the panels. 2D and 3D modelling results from b) from Tschirhart et al., 2013d, c) the dashed line delineates the thrust surface of the SLIC; from Tschirhart et al., 2013b, and d) from Tschirhart et al., 2013a. Hg: Hudson granite; Ms: Martell syenite; SIS: Snow Island Suite; SLIC: Shultz Lake intrusive complex; WLg: Woodburn Lake group; uAb: undifferentiated Archean basement.

Tschirhart *et al.* (2013d) demonstrated the value of partially constrained inversions in the northeastern Amer synform (Figure 4b), a broad fold and thrust belt stretching over 100 km and underlying the central axis of the northeast Thelon Basin. The belt is of interest, as strata-bound uranium occurrences are associated with linear magnetic markers in the Amer group and conductive graphitic units also have the potential to host deposits below the Thelon Formation cover (Davidson and Gandhi, 1989). Near the northeastern end of the Amer synform, sparse exposure resulted in limited structural data and speculative geological interpretations with multiple possible geometric configurations (Calhoun *et al.*, 2014 and references therein). Distinct concentric oval magnetic anomalies in this area form an elongate, aeromagnetic bulls-eye, interpreted as a canoe-shaped synform. Follow-up modelling generated two-dimensional (2D) geometries of synthetic inverse models that mimic the isolated anomaly within the bulls-eye. In the absence of geological controls, the 2D models were incorporated into a reference model, which forms the input in the inversion algorithm (Tschirhart *et al.* 2013d). A major innovation of Tschirhart *et al.* (2013d) was the integration of geophysically derived constraints that maintain structure at depth and verify the concept of a partially constrained inversion (Figure 4b).

The Schultz Lake intrusive complex (SLIC) unconformably underlies the Barrensland Group in the northeast Thelon Basin. To constrain its geometry and framework (Figure 4c) with respect to nearby ore-hosting metasedimentary rocks, Tschirhart *et al.* (2013b) used joint gravity and magnetic forward modelling that incorporated magnetic susceptibility, density, and geological mapping constraints. The SLIC comprises 1.83 Ga Hudson granite and Martell syenite and is expressed on the aeromagnetic map as an abrupt high, cross-cut by intersecting demagnetized fault zones, some of which host uranium deposits in supracrustal enclaves (Hunter *et al.*, 2012). Through an iterative process with project geologists, the data were used to test three hypotheses regarding the shape of the complex. The best-fit model indicates a 200–300 m thick, gently west-dipping, sheet-like body that intruded and encloses highly metamorphosed Neoarchean supracrustal rocks of the Woodburn Lake group (Figure 4c). The composite sheet was modelled as a thrust package structurally emplaced over weakly metamorphosed Neoarchean supracrustal rocks, themselves cut by high-level equivalents of Hudson granite. The timing of the thrust post-dates intrusion of the Hudson granites in both panels.

South of the SLIC and Thelon Basin, Tschirhart *et al.* (2013a) used ground gravity, aeromagnetic, electromagnetic, and remote sensing datasets to constrain the subsurface geological contacts of a basement klippe. Inversions of the magnetic data defined several dyke arrays, and forward modelling defined a deep-seated intrusion interpreted to belong to the 2.6 Ga Snow Island Suite (SIS on Figure 4d; Peterson *et al.*, 2015a; 2015b; 2015c). The forward modelling brought to attention the nature and geometry of broad positive magnetic anomalies associated with Snow Island Suite plutons, some of whose contacts are exposed but others deeply buried. Tschirhart *et al.*, (2013a) presented the first thickness estimate of the pluton. Another widespread manifestation of the Snow Island Suite is as tectonically emplaced, non-magnetic sheets that structurally overlie Neoarchean supracrustal rocks as modelled by Thomas (2012)(Pehrsson *et al.*, 2013) and form the immediate substrate for Paleoproterozoic strata such as the Amer, Ketyet River and Montresor belts (Jefferson *et al.*, this volume).

Closer to the Thelon Basin margins, the location and timing of faults that controlled the development of the basin were explored using a new approach based on the Blakely and Simpson (1986) algorithm as implemented in the geophysical software Geosoft Oasis montaj™. For every magnetic peak, the algorithm calculates a strike and dip direction based on the trend of adjacent maxima and source geometry, respectively. Because the dip direction is a function of the down-slope gradient of the magnetic source body, it is always perpendicular to the strike and pointing away from the magnetic source body. Gridding the dip direction resulted in the definition of blocks of similar magnetic-lithologic character separated by magnetic lineaments marking fault offsets. Used in corroboration with a digital elevation model, these lineaments were matched with surface geological features to deduce fault timing and reactivation (Tschirhart et al., 2013c).

The interpreted structures from Tschirhart *et al.* (2013c) served as input for modelling the basal architecture of the northeast Thelon Basin, as described in Tschirhart *et al.* (2014). Because the sedimentary sequences of the Thelon Basin are non-magnetic, any anomalies within the basin margins are attributed to the underlying basement rocks. Limited drill-hole intersections and sparse seismic refraction data provide the only documented unconformity depths (Overton, 1979), so Tschirhart *et al.* (2014) utilized a combination of automatic and inverse source depth routines to compute depth estimates on idealized source bodies corresponding to known basement units. By constructing numerous intersecting profiles that incorporated all known and calculated depth estimates, a pseudo 3D model of the basin was constructed. The model illustrated a highly variable basement topography, including northwest-trending horst and graben structures and east-northeast- to northeast-trending faults, similar to the uranium-hosting Judge Sisson Fault. The deepest parts of the basin are buried by ~950 m (>2100 m in Tschirhart and Pehrsson, 2016) of siliciclastic strata. The northwest-southeast fault system, termed the Mackenzie fault array by Tschirhart *et al.* (2014) (and subsequently, the Bathurst fault array in Tschirhart and Pehrsson, 2016 and Tschirhart *et al.* 2017), appears to be the dominant set of structures controlling the geometry (and depth) of the basin. Forward modelling of gravity and magnetic data in the southwest Thelon Basin (Tschirhart and Pehrsson, 2016) noted a similar association with northwest-trending structures that primarily controlled basin geometry and the locations of fault-bounded depocenters.

The 3D geophysical interpretations (including forward and inverse modelling products) further allowed for discrimination of the geometry of buried supracrustal packages such as the Amer belt

(Tschirhart *et al.*, 2017). The calibration of magnetic anomalies with rock packages described above allowed for the construction of a map of buried geology predicted by geophysical data (Figures 5a; 5b) in the northeast Thelon Basin (Tschirhart *et al.*, 2017) that served as a training area for additional studies in the southwestern part of the basin (Tschirhart and Pehrsson, 2016). When combined with the pseudo-3D model, the interpretive products identified areas most prospective for unconformity-related uranium mineralization to focus future exploration efforts (Tschirhart and Pehrsson, 2016; Tschirhart *et al.*, 2017). Prospective features include intersecting reactivated faults, fertile basement units, and minimal burial depths, such as the buried intersecting faults northeast of the SLIC and in the central Thelon over interpreted Woodburn Lake group (Figure 5). The results of the broader GEM Uranium project were enabled by integrating multiple geoscientific datasets (Jefferson *et al.*, this volume). Furthermore, the integrated use of geophysics and geology optimized time in the field.

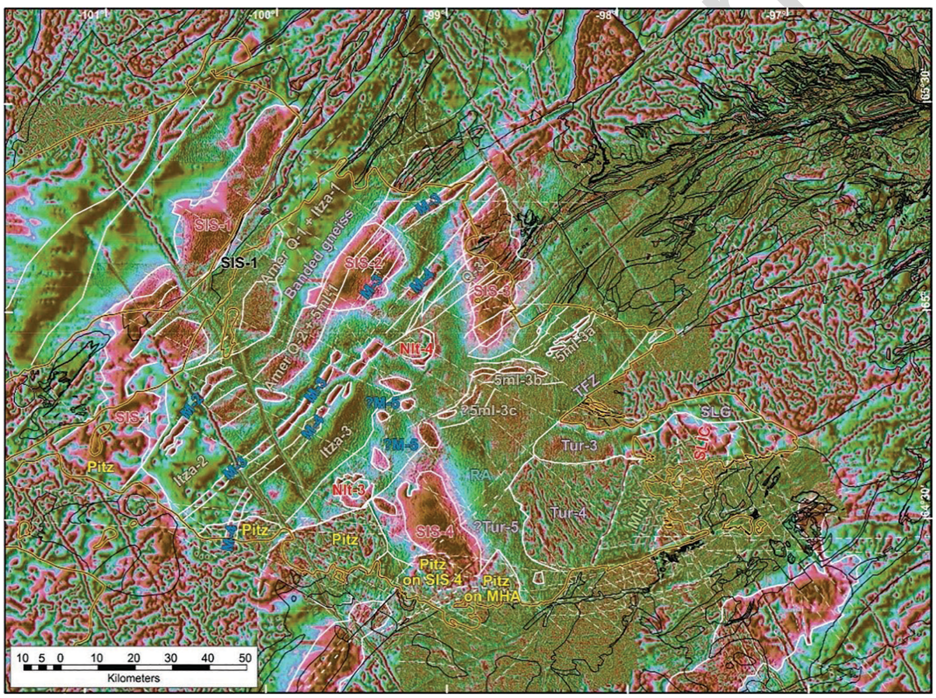

**(a)**

(b)

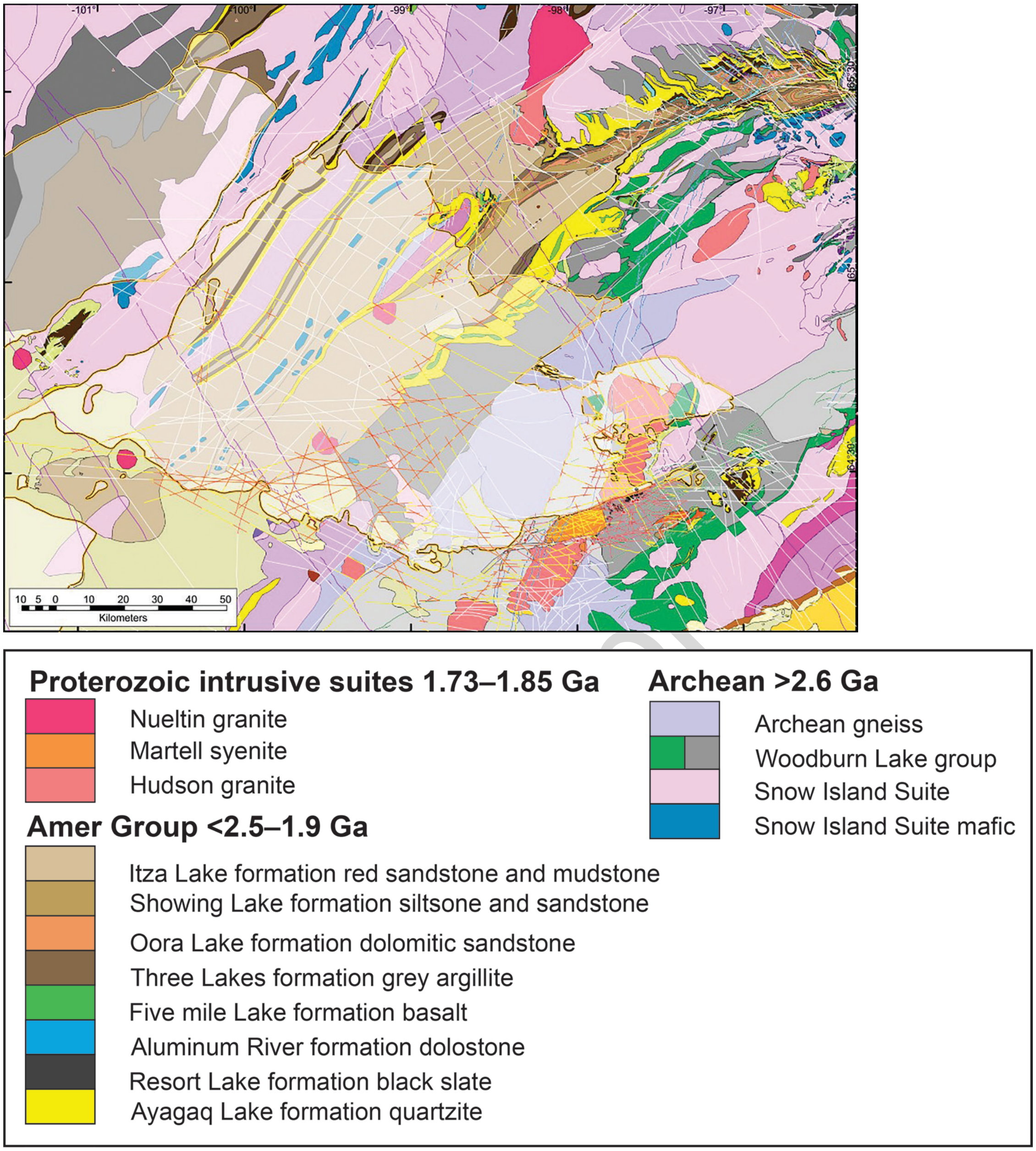


**Figure 5:** a) Enhanced image of the northeast Thelon Basin and surrounding region using tilt derivative displayed at 60% transparency over greyscale Theta. The previously mapped geological contacts and labels outside the Thelon Basin are in black (after Jefferson et al. 2015). Outline of Thelon Formation plotted as thin black line on thick orange line. Select faults plotted as dashed white lines. Newly mapped geophysical units outlined in white are labelled as follows: 5ml – Five Mile Lake formation; Itza – Itza lake formation; Amer Q – Ayagaq lake formation; Nlt – Nueltin granite; MHA – Marjorie Hills Assemblage; SIS – Snow Island Suite; M – mafic intrusive; SLIC – Shultz Lake intrusive complex; TFZ – Turqavik fault zone; Tur – Turqavik; RA – Rumble Assemblage; SLG – Shultz Lake graben. b) Remote predictive map of the geology at the unconformity surface beneath the

Thelon Basin. Surrounding geology is after Jefferson et al. (2015). White lines are selected reactivated faults, yellow lines are reactivated faults within uranium-prospective basement units, and red lines are intersecting reactivated faults in uranium prospective basement units. Colours as in Figure 1 from Tschirhart et al. (2017). Figure from Tschirhart et al. (2017).

## 4. PROJECT AREAS

In the following sections, we briefly review results from selected regions investigated in the western Churchill Province under GEM.

### *4.1 Melville Peninsula*



Located in the eastern part of the region covered in this synthesis, Melville Peninsula of the north Rae craton displays tectonic and geological settings prospective for precious- and base-metal mineralization and diamondiferous kimberlite (Area 1 on Figures 1, 2, 3; Corrigan *et al.*, 2013; Spratt *et al.*, 2013a). Aeromagnetic surveys and three subsequent field seasons of geological mapping resulted in updated geological maps (Table 1; Corrigan *et al.*, 2013), in which Melville Peninsula was divided into four distinct lithotectonic domains: the Archean Northern Granulite, Prince Albert and Repulse Bay blocks, and overlying Penrhyn Group of Paleoproterozoic age. These domains predominantly comprise reworked Archean orthogneiss, Archean and Paleoproterozoic supracrustal belts (Prince Albert Group and Penrhyn Group, respectively), and mafic to felsic plutonic rocks. An abrupt Bouguer gravity gradient in the regional data marks the domain boundary between the Northern Granulite block, a prominent Bouguer gravity high, and the Prince Albert block (dashed line separating NGb and PAb on Figure 6a). Like much of the Rae craton, the dominant magnetic fabric strikes northeast, likely reflecting Paleoproterozoic reworking during the Trans-Hudson orogeny (Figure 2; Berman *et al.*, 2005; 2015; Corrigan *et al.*, 2013).

The Prince Albert and Repulse Bay blocks are separated by high strain rocks of the Lyon Inlet boundary zone (LIBZ on Figures 6a, 6b). On the aeromagnetic map, the boundary zone is the northern limit of curvilinear, east-northeast-striking positive magnetic anomalies (not shown here, but Figure 2b in LaFlamme *et al.*, 2014). This zone coincides with a near-vertical, low-resistivity magnetotelluric anomaly (Spratt *et al.* 2013a). Spratt *et al.* (2013a; 2014) also noted a change in the mantle structure or composition (see also Snyder *et al.*, 2015; Liu *et al.*, 2016) between these two blocks, coinciding with the surface trace. This boundary has alternatively been interpreted as a Neoarchean suture zone (Skulski *et al.*, 2014), an exhumation-related structure accommodating uplift of the deep-crustal

Repulse Bay block (Laflamme *et al.*, 2014, 2017), or an older feature reactivated in the Proterozoic (Peterson *et al.*, this volume).

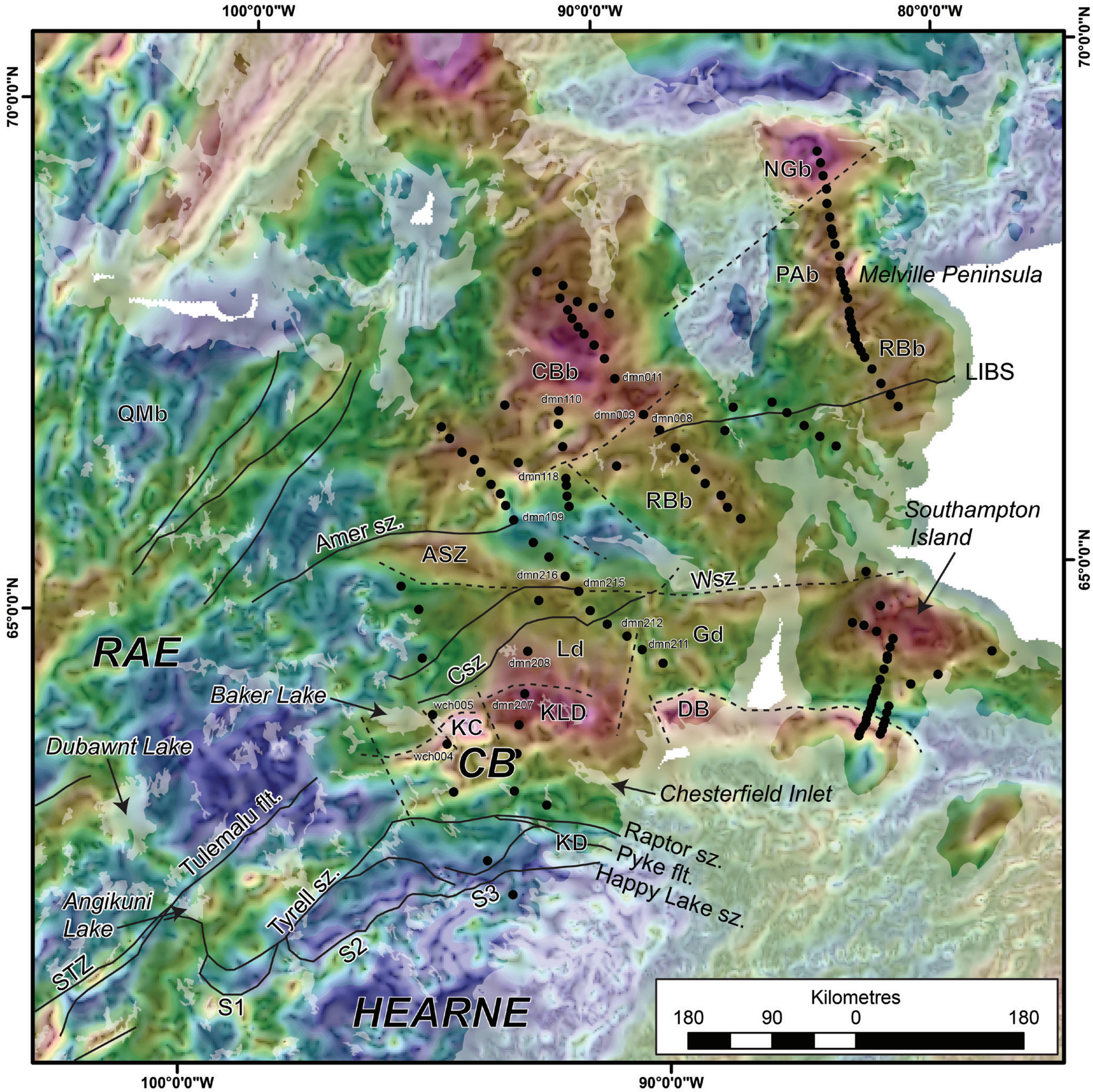


**Figure 6a:** Horizontal gradient magnitude of the Bouguer gravity anomalies displayed at 50% greyscale transparency over the isostatic residual Bouguer gravity data. Solid black lines represent select major faults from Tella et al. (2007), Pehrsson et al. (2014b), and Skulski et al. (2017). Block dots are MT stations and labels, as discussed in the text. Dashed black lines represent interpreted structures and domain boundaries discussed in text. ASZ = Amer shear zone; CB = Chesterfield block; CBb = Committee Bay block; Csz = Chesterfield shear zone; DB = Daly Bay; Gd = Gordon domain;

KC = Kramanitaur Complex; KD = Kaminuriak domain; KLD =Kummel Lake Domain; Ld = Lunan domain; LIBZ = Lyon Inlet boundary zone; PAb = Prince Albert block; NGb = Northern Granulite block; QMb = Queen Maud block; RBb = Repulse Bay block; Wsz = Wager shear zone. S1, S2, S3 = possible southern limits of the Chesterfield block (Berman et al., 2007).

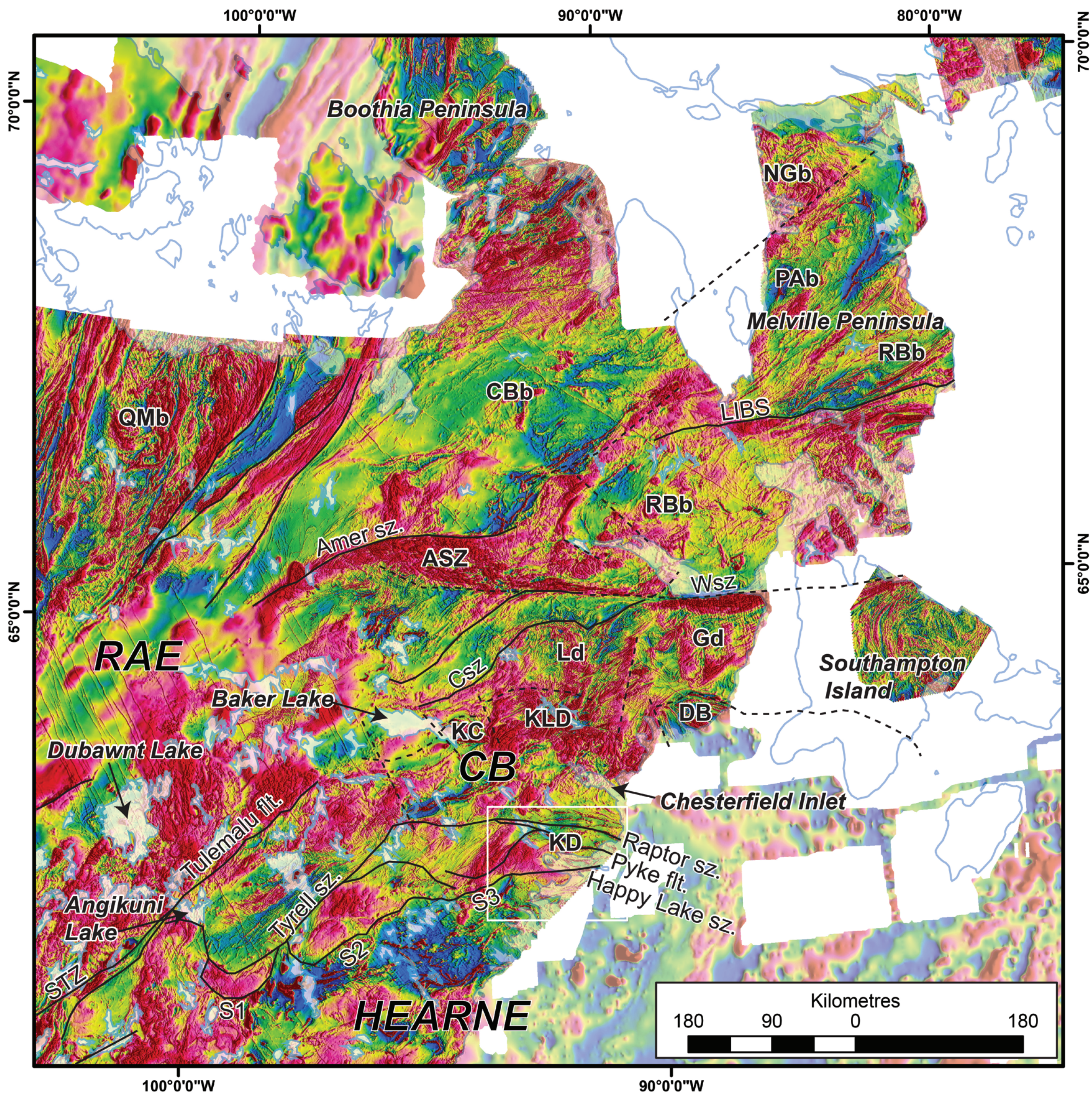


**Figure 6b:** Residual total field. Solid black lines represent select major faults from Tella et al. (2007), Pehrsson et al. (2014b), and Skulski et al. (2017). Block dots are MT stations and labels, as discussed in the text. Dashed black lines represent interpreted structures and domain boundaries discussed in

text. ASZ = Amer shear zone; CB = Chesterfield block; CBb = Committee Bay block; Csz = Chesterfield shear zone; DB = Daly Bay; Gd = Gordon domain; KC = Kramanitaur Complex; KD = Kaminuriak domain; KLD =Kummel Lake Domain; Ld = Lunan domain; LIBZ = Lyon Inlet boundary zone; PAb = Prince Albert block; NGb = Northern Granulite block; QMb = Queen Maud block; RBb = Repulse Bay block; Wsz = Wager shear zone. S1, S2, S3 = possible southern limits of the Chesterfield block (Berman et al., 2007). White outline is area shown in Figure 7.

### *4.2 Boothia Peninsula and Somerset Island*

The Boothia Peninsula-Somerset Island region is located in the northwestern part of the synthesis region (Table 1; Area 2 on Figures 1, 2, 3 ). Magnetic lows and subdued responses on the aeromagnetic map are predominantly correlated with non-magnetic belts of metasedimentary rocks that are cross-cut by curvilinear, high-amplitude magnetic highs corresponding to intermediate to mafic metaplutonic rocks (Sanborn-Barrie *et al.*, 2018). Magnetic susceptibility measurements (Ugalde unpublished data, 2018) indicate that high magnetic susceptibility values correspond to mafic intrusive rocks, whereas felsic and intermediate intrusive rocks have similar, lower values. Polyphase deformation is widespread across the region and this is reflected in the magnetic patterns as abrupt truncations, lateral displacement, attenuation effects, and curvilinear fold interference patterns (Sanborn-Barrie *et al.*, 2018). Boothia Peninsula is transected by the regional, southwest-striking, moderately northwest-dipping Sanagak Lake shear zone that extends at least 160 km (Sanborn-Barrie *et al.*, 2018; 2019a).

### *4.3 Thelon Tectonic Zone*

Separating the Rae craton from the Slave craton in the east, the Thelon tectonic zone (TTZ) Area 3 on Figures 1, 2, 3) has been considered to represent (a) a 2.03–1.96 Ga arc prior to the Slave-Rae collision (Hoffman, 1988) or (b) an intracratonic mountain belt formed subsequent to Slave-Rae accretion (Chacko *et al.*, 2000; Schultz *et al.*, 2007). Geophysically, the TTZ comprises a series of north- to north-northeast-trending magnetic lineaments that extend 550 km from the McDonald Fault to north of the Queen Maud Gulf (Table 1; Figure 2, box 3; Berman *et al.*, 2016; 2018). The detailed nature of the interaction between the Slave and Rae cratons remains elusive, and the crustal architecture poorly understood. Owing to the paucity of bedrock exposure, the aeromagnetic surveys were key in outlining high amplitude, linear anomalies corresponding to *ca.* 2.0 Ga Western, Central, and Eastern plutonic belts (Survey 3a on Figure 2) of magmatic arc geochemical character (Whalen *et al.*, 2018), as well as a non-magnetic, *ca.* 1.90 Ga leucogranite belt, and the margins of the Slave and

Rae cratons (Berman *et al.*, 2018). Subtle features in the high-resolution data over the western plutonic belt outline a curvilinear anomaly corresponding to a quartz diorite to monzogranite suite that overlaps the boundary with the Slave craton (Berman *et al.*, 2018). The aeromagnetic data further aided the interpretation of intersecting the TTZ structures with those of the Bathurst fault system (Ma, 2018), which extends northeastward beneath the Thelon Basin. There, Ma (2018) documented progressive strain localization and fluid-rock interaction, which are important for mobilizing and localizing hydrothermal fluid flows (Ma, 2018; Ma *et al.*, 2019).

Two regional magnetotelluric transects provided constraints on the geometry of the Slave-Rae boundary at depth (Roberts *et al.*, 2015; locations shown as black dots within Area 3 on Figure 3). 3D inversion results suggested an east-dipping Rae- Slave boundary, consistent with Nd-Sm isotopic variations (Berman *et al.*, 2018). However, within the crust the geometry is complex (Roberts *et al.*, 2015; Berman *et al.*, 2018). In the Rae craton, the upper 10 km of the conductivity cross-section is correlative with resistive, *ca.* 2.0–1.90 Ga plutonic rocks, such as leucogranite. Below 10 km, the Rae craton is underlain by highly conductive zones, interpreted to reflect either deeply buried metasedimentary rocks or alternatively, graphite-grain boundary films developed during granulite-facies metamorphic conditions (Roberts *et al.*, 2015). An upper crustal high-conductivity region underlying the Ellice River supracrustal belt may reflect sulphide enrichment also documented in stream sediment surveys (McCurdy *et al.*, 2013; Berman *et al.*, 2018). Beneath the Slave craton, the lower crust (>20 km depths) appears to be more resistive than corresponding levels in the Rae (Roberts *et al.*, 2015). Taken together, the geophysical data indicate steep structures and complex geometry resulting from multiple intrusive, metamorphic and deformational events.

***4.4 Montresor Belt***

Paleoproterozoic Montresor group metasedimentary rocks occur in a narrow syncline about 100 km north of the Amer group (Area 4 on Figures 1, 2, 3), with which they have been correlated (Rainbird *et al.*, 2010; Percival *et al.*, 2017). Magnetic marker horizons outline structures in the belt and are similar to those documented in the Amer group (Tschirhart *et al.*, 2013d; Tschirhart *et al.*, 2017; Percival and Tschirhart, 2017). Elevated levels of copper, silver, and gold were identified in a hydrothermal breccia within the syncline, the first example of this mineralization style recognized in the region (Percival *et al.,* 2015). To determine the spatial extents and subsurface geometry of the demagnetized hydrothermal breccia, Tschirhart *et al.* (2015) derived the apparent susceptibility from the magnetic data using an approximate method. These approximate values on the syncline limbs were scaled using sparse magnetic susceptibility measurements from outcrops. The scaled apparent susceptibility values served as constraints for magnetic forward models that illustrated the geometry of the limbs and demagnetized zones, including a narrow vertical zone extending from the surface exposure of the hydrothermal breccia. Forward modelling of the regional gravity data in Tschirhart *et al.* (2015) further recognized an extensional detachment (and potential metamorphic core complex) corresponding to the Amer shear zone. This study was expanded in Percival and Tschirhart (2017) where five additional forward models were constructed across the northeastern syncline (Figure 5 in Percival and Tschirhart, 2017). By graphically restoring the limbs of the late syncline to their pre-$F_3$ state, forward models revealed early ($D_1$) thrusts and later ($D_2$) extensional faults, the latter related to the late-orogenic extensional phase of the Trans-Hudson orogeny (Percival *et al.*, 2015; 2017; Percival and Tschirhart, 2017). Tschirhart *et al.* (2015) postulated that depending on timing, the extensional event that exhumed the interpreted core complex could have controlled the geometry of the deposition of the 1.85–1.50 Ga Dubawnt Supergroup, distributed in northeast-trending fault-bounded troughs, consistent with the interpretations of Hadlari and Rainbird (2011).

### *4.5 Tehery Lake and Wager Bay*

Southwest of Melville Peninsula, the Tehery Lake-Wager Bay area (Table 1; Area 5 on Figures 1, 2, 3) is dominated by Meso- to Neoarchean gneissic rocks, folded Archean and Paleoproterozoic supracrustal belts, and felsic to ultramafic plutonic rocks belonging to several plutonic suites, including the *ca.* 2.6 Ga Snow Island, *ca.* 1.85–1.80 Ga Hudson, and *ca.* 1.83–1.82 Ga Martell suites (Wodicka *et al.*, 2016, 2017; Steenkamp *et al.*, 2015, 2016; Peterson *et al.*, this volume). The STZ has been historically interpreted to transect the southern portion of the project area based on potential field anomalies that suggest highly magnetic, dense rocks (Hoffman, 1988). Bedrock mapping, combined with surficial studies, identified potential for base- and precious-metal mineralization, primarily in the Archean supracrustal rocks in the vicinity of the Chesterfield shear zone, and diamondiferous kimberlite outside previously known kimberlite fields (Wodicka *et al.*, 2016; Steenkamp *et al.*, 2015; McMartin *et al.*, 2019 and references therein). In addition to redefining the distribution of Archean versus Paleoproterozoic supracrustal rocks in complexly deformed regions, this work documented the style and deformation of major Paleoproterozoic structures, including the Wager Bay and Chesterfield shear zones (Tschirhart *et al.*, 2016; Wodicka *et al.*, 2017; Therriault *et al.*, 2017). Furthermore, new geophysical maps (Figures 3, 6a, 6b) illustrate that gravity highs in the southern Tehery Lake-Wager Bay region do not correspond to geometrially consistent structures as would be predicted for the originally defined STZ. Rather, inverse models of the regional gravity data illustrate that the granulite-facies Daly Bay and Kummel Lake domains, bordering Chesterfield Inlet and Hudson Bay, have different subsurface geometries (Wodicka *et al.*, 2017). Whereas the ca 1.9 Ga Daly Bay complex is carried on a steep east-dipping thrust, the Kummel Lake domain is modelled as dipping northwards below amphibolite-facies gneissic rocks, resembling a metamorphic core complex. A linear structure visible on both the upward continued magnetic data and regional gravity data, demarcates the boundary between the isotopically distinct Gordon and Lunan domains (Wodicka *et al.*, 2017; Figure 6a, 6b). On a more detailed scale, source depth routines and forward models of the modern aeromagnetic data in the Gordon domain allowed the geometry of the 2.6 Ga Borden Complex, a compositionally distinct Snow Island pluton, to be defined as sheet-like (Wodicka *et al.*, 2017; Peterson *et al.*, this volume).

Magnetotelluric investigations in the Tehery Lake region are described by Spratt *et al.* (2014). Three regional profiles indicate generally resistive upper crust and conductive lower crust but provide relatively sparse definition of upper crustal features in the Wager-Tehery region.

### *4.6 Southampton Island*

Southampton Island in northwestern Hudson Bay (Area 6 on Figures 1, 2, 3) is underlain predominantly by high-grade gneiss, mainly of plutonic origin with subordinate metasedimentary units, as well as sparse mafic-ultramafic intrusions (Berman *et al.*, 2011; Sanborn-Barrie *et al.*, 2014b). Paleozoic strata cover the southwestern part of the island. Where exposed, shield rocks are dominated by curvilinear magnetic anomalies (Figure 2) and a positive gravity response (Figure 3) that characterize Mesoarchean to Paleoproterozoic plutonic and supracrustal rocks that were intensely deformed together and refolded at the crustal scale. South of the Wager shear zone (Figure 6b), Southampton Island displays a discontinuity between magnetic anomalies over the Precambrian plutonic-dominated basement exposed in the eastern half of the island and the region covered by Paleozoic sedimentary rocks to the southwest (Spratt *et al.*, 2012b; Figure 1). To image potential crustal-scale structures that explain the discontinuity, long period and broadband magnetotelluric data were collected to examine the deep lithosphere (Spratt *et al.*, 2012b). The authors observed more complex structures in the upper crust below the Paleozoic cover, including a narrow east-trending resistive crust that they correlated with mafic granulite-facies rocks exposed in a small window in the southwest. The authors and Spratt *et al.* (2014) follow Hoffman (1988) and Gordon and Heywood (1987) in correlating this discontinuity with the Daly Bay complex to the west. Strong, west-northwest-striking magnetic and gravity anomalies support this interpretation. Spratt *et al.* (2012b) further noted northward thickening of Rae crust from ~30 km below Southampton Island to ~40 km below Melville Peninsula, consistent with tectonic models that propose southeastward underthrusting of Rae mantle beneath a wedge of Meta Incognita microcontinent exposed on southern Baffin Island (Figure 1; Corrigan *et al.*, 2009; Berman *et al.*, 2013b; Snyder *et al.*, 2013).

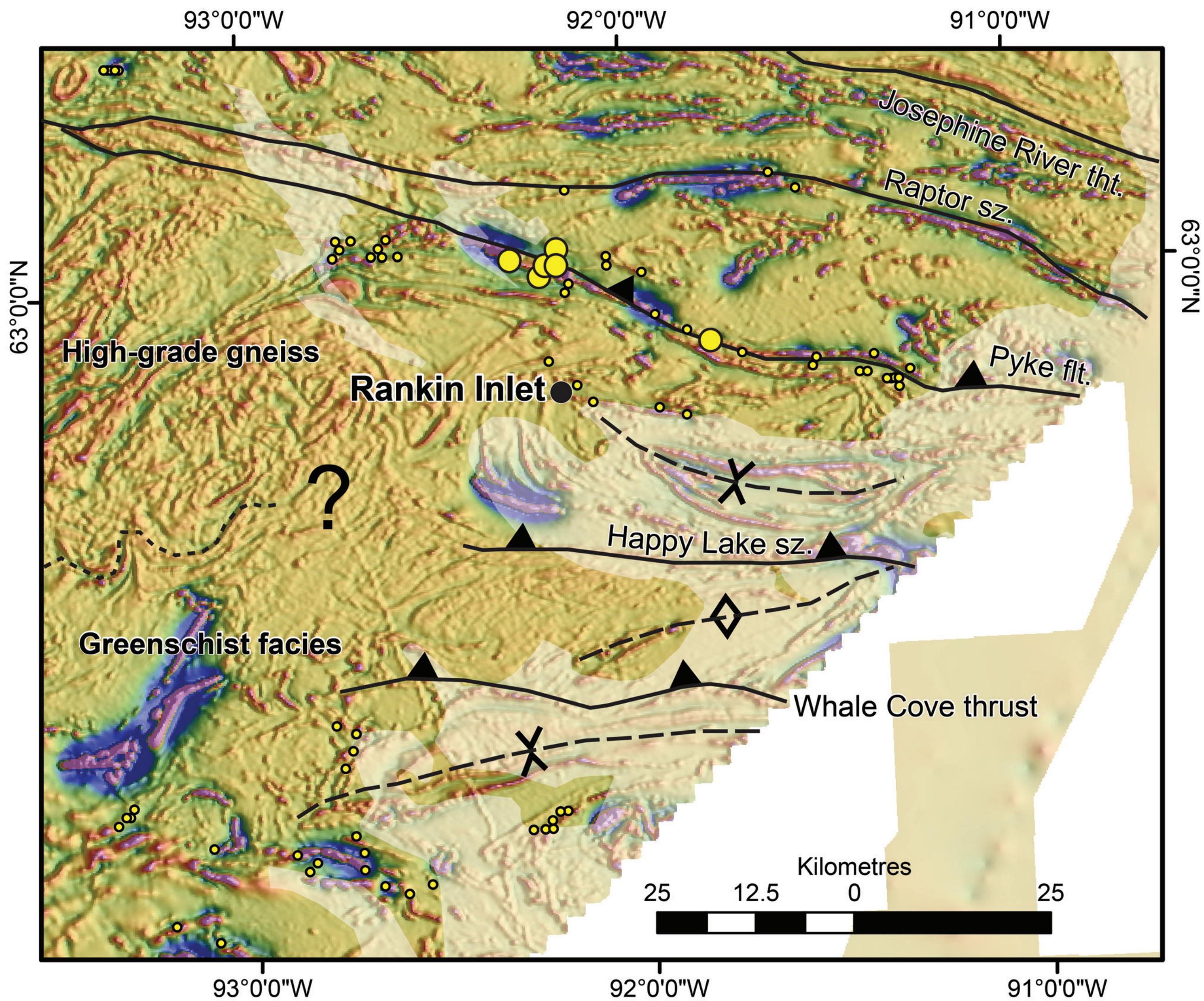


**Figure 7:** First vertical derivative of the magnetic field of the Rankin Inlet area showing the distribution of gold deposits (large yellow circles), and occurrences and showings (small yellow circles) in relation to faults and shear zones (solid black lines), and folds (dashed black lines), (after Pehrsson et al., 2014a).

### *4.7 Chesterfield Inlet*

Particularly extensive drift cover obscures complex bedrock features in the Chesterfield Inlet area (Area 7 on Figures 1, 2, 3) that nevertheless has been the focus of extensive gold exploration. Upgraded aeromagnetic coverage has facilitated geological interpretation relevant to both regional scale Churchill architecture and mineralized structures (Table 1; Figures 6b, 7; Pehrsson *et al.*, 2014a). The Chesterfield block was recognized as a tectonic entity by virtue of its distinct units (Sandeman *et al.*, 2006; Acosta-Gongora *et al.*, 2018), and deformation history involving accretion to the margin of the Rae craton prior to 2.61 Ga (Berman *et al.*, 2007 and references therein). These rocks underwent additional deformation at 2.56–2.50 Ga (Davis *et al.*, 2006) and deposition of Paleoproterozoic sedimentary and volcanic rocks (Lawley *et al.*, 2016), prior to amalgamation with the Hearne at *ca.* 1.91 Ga and reworking at 1.85 Ga (Davis *et al.*, 2006). Integration of the regional high-resolution aeromagnetic data with previous structural and stratigraphic studies outlined a new feature—the Kaminuriak domain, which underlies the most heavily drift-covered region. It is characterized by curvilinear magnetic features defining large refolded folds with 20–70 kilometre long axial surfaces. This pattern is structurally bounded by the Raptor shear zone to the north and the Happy Lakeshear zone to the south (Figure 6b). Combining recent geological results near Rankin Inlet (Lawley *et al.*, 2015, 2016), Happy (Berman *et al.*, 2007) and Yathkyed (Acosta-Gongora *et al.*, 2018) lakes illustrates that the Kaminuriak domain comprises Chesterfield block Archean and Paleoproteorzoic crust that is transposed and regionally folded during late extrusion and south-vergent thrusting of the domain over the Hearne craton (Pehrsson *et al.*, this volume).

Orogenic gold deposits, occurrences and showings of the Chesterfield Inlet area are hosted by Archean volcano-sedimentary units along prominent shear zones, particularly the Pyke fault (Figure 7; Carpenter *et al.*, 2005). Faults and shear zones have protracted deformation histories culminating in reactivation and mineralizing fluid ingress between 1.9 and 1.85 Ga (Carpenter and Duke, 2004; Lawley *et al.*, 2015). Current exploration models for the region identify the Chesterfield block and Rae Archean supracrustal packages, along with reactivated shear zones, as key elements in gold prospectivity (Pehrsson *et al.*, 2013, 2014a; Lawley *et al.*, 2015; Janvier et al, 2015). Significantly, the Chesterfield aeromagnetic survey illustrates that the Pyke break is a splay to the Raptor shear zone that bounds the Kaminuriak domain to the north (Figures 6b, 7). Such second-order structural features are commonly considered the most prospective for orogenic gold mineralization (Goldfarb *et al.*, 2005; Dubé *et al.*, 2015).

### ***4.8 South Rae***

South of the western Thelon Basin, preliminary studies in the south Rae region (Area 8 on Figures 1, 2, 3) documented unrecognized mineral potential in a particularly poorly understood part of Churchill province that had previously only been mapped during early GSC reconnaissance (1:500,000 to 1:2.5 M scale; Harris *et al.*, 2013 and references therein). A modern aeromagnetic survey (Table 1) tied to similar surveys in adjacent mapped parts of northern Saskatchewan and southeast Northwest Territories allowed completion of 1:250,000 scale maps in three field seasons (e.g. Martel *et al.*, 2018). In conjunction with bedrock mapping, the integrated aeromagnetic coverage enabled distinction of six geophysically and isotopically defined domains, named Porter, Boomerang, Penylan, McCann and Firedrake, each with a characteristic magmatic and 2.6–1.80 Ga tectono-metamorphic history (Percival *et al.*, 2016; Martell *et al.*, 2018; Regis *et al.,* 2017; Thiessen *et al*., 2020; Martel *et al.*, this volume) and transected by sparse dyke swarms (Mowbray and Pehrsson, 2019). The domains strike predominantly northeast and notably display distinctive aeromagnetic signatures that reflect the variable intensity of moderate- to high-pressure, crustal scale reworking during the Snowbird and Trans-Hudson orogenic phases. The characteristic geophysical expression of several domains allow correlation with other parts of the Rae craton-Chesterfield block. For instance, the McCann domain and its *ca.* 2.55 Ga metasedimentary rocks that were metamorphosed and deformed during the *ca.* 2.3 Ga Arrowsmith Orogeny are characterized by the same widespread smooth magnetic low as the contemporaneous Sherman basin of the Queen Maud block (Schultz *et al.*, 2007). Similarly, the Firedrake domain displays the same large, regional, complex refold pattern of distinctly linear magnetic features that is observed in the Kaminuriak domain (Figure 6b). Both are significant regions that were exhumed from the mid-crust during late Trans-Hudson time (Martel *et al.*, 2018), suggesting that this pattern may stem from crustal flow processes during extensional collapse of an orogenic plateau (Regis et al., 2021).

The individual geologic domains of South Rae are bounded by extensive, newly recognized ductile and brittle-ductile shear zones that correspond to textural discontinuities on the magnetic maps and derivative products (shown in Jamison, 2018; Thiessen *et al.*, 2018; and Martel *et al.*, 2018). Several of these boundary zones are spatially associated with rare earth element (REE)-prospective syenite bodies (Jamison *et al.*, 2017).

### *4.9 Athabasca Basin*

The Athabasca Basin (Area 9 on Figures 1, 2, 3) in the southern part of the synthesis area hosts world-class uranium deposits and is the premier exploration region in Canada for unconformity-associated uranium deposits (Jefferson and Delaney, 2007). Non-magnetic sedimentary rocks cover the majority of the deposits, such that aeromagnetic surveys, coupled with other multiparameter geophysical transects, are essential to interpreting the geology of the crystalline basement that hosts the uranium deposits. To maximize resolution, systematic airborne magnetic and radiometric surveys were completed to modern standards (Table 1) over the Saskatchewan portion of the Athabasca Basin, in collaboration with Saskatchewan Industry and Resources, resulting in the largest contiguous modern aeromagnetic and radiometric dataset in Canada (Card *et al.*, 2010). In 2017, through the Targeted Geoscience Initiative (TGI) Uranium project, the coverage was expanded to include the southwestern Athabasca Basin (Box 9d on Figure 2; Table 1), including parts of Alberta and south of the basin margins. The Athabasca Basin geophysical compilations provided fundamental information for industry operating in the basin to help assess the uranium resource potential of areas buried by Athabasca Supergroup cover. In conjunction with drill core information and rock property information, improved resolution in the southwestern Athabasca Basin allowed for redefinition of the location and distribution of felsic intrusive bodies, and identified several major crustal structures that may have played a role in localizing hydrothermal fluid movement (Figure 8; Tschirhart *et al.*, 2019; 2020). Moreover, the airborne magnetic surveys showed discrete, isolated circular anomalies (Kiss and Tschirhart, 2017) that have the potential to correspond to kimberlite pipes.

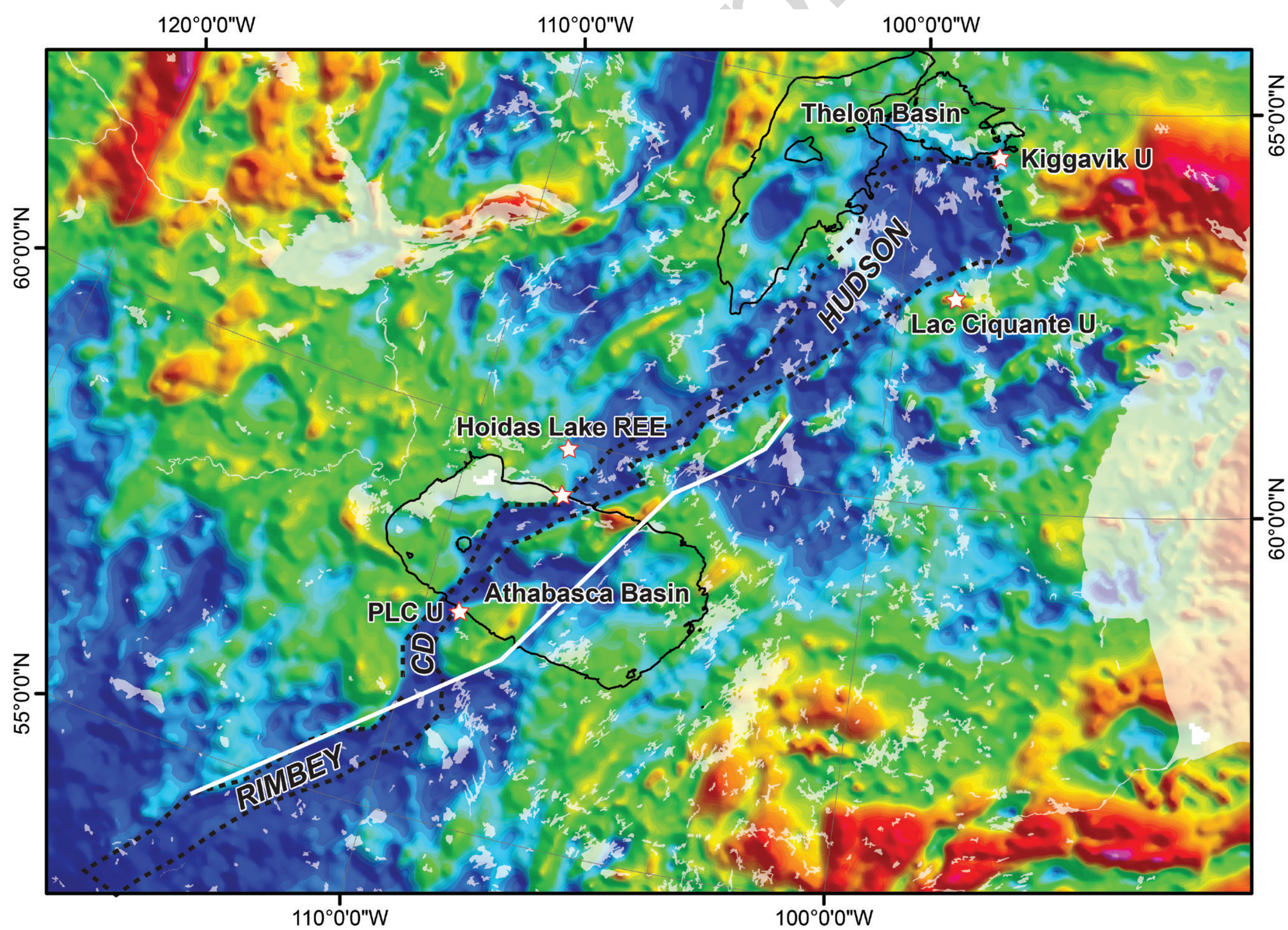

**Figure 8:** Location of uranium and REE deposits and occurrences over the Bouguer gravity. Thelon and Athabasca basins outlined in black. White line delineates location of mapped STZ; dashed black lines outlines Bouguer gravity low.

## 5.0 DISCUSSION

Geophysical information is used most effectively to constrain geological models. These connect through rock physical properties, and models will continue to improve as the rock property database expands. Geophysical methods provide essential depth constraints on 3D geological models, whether illuminating crystalline bedrock through a thin veneer of glacial sediments, thicker sections of Proterozoic strata or Phanerozoic cover, or imaging crust- or lithosphere-scale features. Over the decades as regional aeromagnetic coverage became available for the western Churchill region, geophysics has contributed to definition and resolution of geological problems at a range of scales. During the GEM program, acquisition and interpretation of high-resolution aeromagnetic surveys were integral components of a modern geoscientific approach. In the following sections, we highlight the impact of geophysical insights into the evolving picture of geological evolution and the inexorably linked enterprise of mineral exploration. However, domain-by-domain analysis may be required to take account of the protracted and variably reworked nature of the Rae craton, which limits the applicability of data from adjacent domains and adds layers of complexity to interpretations.

### *5.1 Rae Craton Boundaries*

The western and southeastern boundaries of the Rae craton are exposed in the northwestern Canadian shield and were investigated by GEM projects. Gibb and Thomas (1977) first drew attention to the gravity signature of the Slave-Churchill boundary, localized along the TTZ. Their interpretation of higher density Churchill crust led Hoffman (1988) to propose an exhumed Thelon-age Rae plateau, the Queen Maud block. Debate on the nature of this boundary has grown with acquisition of new information, including models involving an intracontinental magmatic belt (Thompson, 1989; Chacko *et al*., 2000). Recent work integrating new geophysical and bedrock mapping illustrates a complex 2.06–1.9 Ga tectono-magmatic history of continental arc magmatism at a consuming margin (Berman *et al*., 2016; 2018; Whalen *et al*., 2018). This boundary is characterized by steeply dipping conductive zones that extend through the crust, however their origin as graphitic metasedimentary layers or high-grade metamorphic zones is uncertain (Roberts *et al*., 2015).

The northern extension of the TTZ is poorly constrained beneath Paleozoic cover and water. Previous extrapolations projected the TTZ through Boothia Peninsula-Somerset Island (Figure 6b;

Wheeler *et al*., 1996), however recent work (Sanborn-Barrie *et al*., 2018) excludes this possibility, requiring a more westerly trajectory through an area of sparse geophysical coverage.

At its southeastern margin, the Rae craton is bordered by the STZ, defined originally as a line of gravity and magnetic anomalies and interpreted as a suture within the Churchill Province (Walcott and Boyd, 1971). Hoffman (1988) inferred the zone to be the Paleoproterozoic boundary between the Archean Rae and Hearne cratons. The STZ can be traced from southern Alberta (Pilkington *et al*., 2000) to the Angikuni Lake area (Figures 6a, 6b). Over much of this length it is expressed geophysically as a chain of positive gravity anomalies corresponding to granulite-facies granitoid gneiss intruded by gabbro-anorthosite, typical of mid to lower crust (Gordon and Lawton, 1995; Sanborn-Barrie *et al*., 2001; Berman *et al*., 2007; Mills *et al*., 2007; Sanborn-Barrie et al., 2019b), although recent studies demonstrate that high-pressure rocks of the Snowbird orogeny occur far to the west of the STZ as originally defined (Regis *et al*., 2019; Martel *et al*., this volume). The magnetic anomalies from Angikuni Lake to Baker Lake are subdued in comparison to the anomalies north of the Tulemalu fault by the overlapping Baker Lake basin, which contains low-density sedimentary and igneous rocks (Figure 2; Tschirhart *et al*., 2013b; 2017; Peterson *et al*., 2015c). The northern dense and highly magnetic features north of Baker Lake along Chesterfield Inlet (Figures 6a, 6b) originally ascribed to the STZ have more recently been shown to be of differing age and origin (Gordon and Lawton, 1995; Sanborn-Barrie *et al*., 2001; Berman *et al*., 2007; Mills *et al*., 2007; Sanborn-Barrie *et al*., 2019b).

A joint magnetotelluric-teleseismic profile detailed deep structural discontinuities supporting juxtaposition of the two terranes (Jones *et al*., 2002). Structural-petrological studies at the southwestern exposures of the STZ in Saskatchewan (Hanmer *et al*., 1995; Mahan and Williams, 2005) have been interpreted as indicative of Archean assembly; however, subsequent work has revealed a complex interface consistent with ca. 1.9 Ga assembly during the Snowbird accretionary phase of the Trans-Hudson orogeny (Berman *et al*., 2007; Thiessen *et al*., 2018).

Several GEM projects provide insight into the enigmatic northeastern extension of the Snowbird zone east of Dubawnt Lake where it lacks a pronounced magnetic and gravity signature (Figure 6a). Several interpretations of its eastern extents have emerged in the Chesterfield-Wager Bay region (Jones *et al*., 2002; Berman *et al*., 2007; Spratt *et al*., 2012b), where relationships among shear zones, exhumed high-pressure rocks, layered igneous complexes and terrane architecture are complex (Spratt *et al*., 2014; Skulski *et al*., 2018) and only separable from older (2.6, 2.55 Ga) and younger (1.85 Ga) structures and events by detailed geochronological work (e.g., Thiessen *et al*., 2018; Sanborn-Barrie *et al*., 2019b; Regis *et al*., 2019). Recent interpretations place the STZ along the major west-dipping Tyrell shear zone (Berman *et al*., 2007; Figures 6a, 6b). Comparison of Figures 2, 3 (Area7), and 6a shows a zone of linear, positive anomalies (Figure 6a - S1, S2, S3) on the most southerly of Berman *et al*. (2007)'s proposed trajectories, coincident with the southern margin of the Kaminuriak domain. A subtle break in the mantle and crust resistivity subjacent to anomaly S3 was modelled in an early MT profile (Jones *et al*., 2002), and is supported by more recent MT models (Figure 11d of Spratt *et al*., 2014), as well as teleseismic definition of their eastward extension in Hudson Bay (Gilligan *et al*., 2016; Liddell *et al*., 2018).

In the sparsely exposed Chesterfield Inlet-Wager Bay region, elucidation of the complex fault geometry and its association with lode gold showings and deposits was enabled by field observations guided by high-resolution aeromagnetic maps (Pehrsson *et al*., 2014a; Wodicka *et al*., 2017). Similarly, gravity profiles defined the 3D geometry of granulite complexes and some shear zones (Tschirhart *et al*., 2016), contributing to regional kinematic analysis. The emerging picture of Snowbird tectonism involves a 1.9 Ga collision between the Rae-Chesterfield craton, whose ca. 200-km-wide southeastern margin underwent burial, structural-metamorphic reworking, and variable compressional and extensional exhumation during accretion of the relatively intact Hearne craton (Pehrsson *et al*., this volume).

***5.2 Internal Rae architecture***

Most of the Rae craton is characterized by a pervasive northeast-oriented structural grain evident in the aeromagnetic data (Figure 2), attributed to the cumulative effects of the Trans-Hudson and older deformation events. While some internal domains of the Rae have distinct aeromagnetic and/or gravity expressions, other, more structurally overprinted domains have more cryptic boundaries, evident only through contrasting isotopic character (Peterson *et al*., 2010; Regis *et al*., 2019; Kellett *et al*., 2020). Conversely, some prominent linear aeromagnetic features correspond to ductile shear zones of relatively minor tectonic significance.

The south Rae region represents a distinct structural style in which shear zones separate domains of variable aeromagnetic intensity and amplitude (Pehrsson *et al*., 2014b; 2015; Percival *et al*., 2016). The shear zones are commonly curvilinear, ductile and brittle-ductile structures of low magnetic intensity that were active between ca. 1.9 and 1.8 Ga (Regis *et al*. 2017; 2019; 2021; Kellett *et al*., 2020). Based on the variable metamorphic ages and pressures of individual domains, the shear zones appear to represent discontinuities among blocks with different burial and exhumation histories (Regis *et al*., 2017; 2021; Thiessen *et al*., 2018). Although most domains consist predominantly of Archean (ca. 2.6 Ga) rocks, some (e.g. Porter, Boomerang) underwent minor Paleoproterozoic reworking, whereas McCann shows a strong Arrowsmith (2.4–2.3 Ga) overprint, Firedrake exhibits a strong Trans-Hudsonian (1.85 Ga) resetting and Snowbird domain, a thorough Snowbird (1.9 Ga) structural-metamorphic reworking (Regis *et al*., 2017, 2019, 2021).

Structural style in the central Rae region is dominated by the superimposed effects of the Snowbird and Trans-Hudson events. The Rae cover sequence, deposited between the Arrowsmith and Snowbird events, acts as a monitor of internal Rae strain. Structural studies of these rocks, in concert with aeromagnetic interpretation, have illustrated a polyphase fold and thrust belt geometry and associated ca. 1.83 Ga high-temperature, moderate pressure metamorphism (Patterson, 1986; Pehrsson *et al*., 2013; Calhoun *et al*., 2014; Percival and Tschirhart, 2017; Dziawa *et al*., 2019), locally superimposed by late extensional structures (Percival *et al*., 2015; Wodicka *et al*., 2017). The regional pattern of individually isolated Rae cover outliers, separated by broad granitic and granulitic massifs west of the Committee Bay-Woodburn greenstone belts, may reflect these late Trans-Hudson structures, including a ductile phase of movement on the prominent Amer shear zone.

To the northeast, the Committee Bay belt is characterized by northeast trending, southeast dipping structures (Figure 6b) and ca. 1.86–1.82 Ga metamorphism (Sanborn-Barrie *et al*., 2014a) that overprint ca. 2.35 Ga fabrics attributed to the Arrowsmith orogeny. In the adjacent Tehery-Wager region to the east, polydeformed sequences represent penetrative Trans-Hudson deformation superimposed on Archean structures. Domains of contrasting metamorphic grade (e.g. Kummel Lake and Daly Bay) are bounded by continuous lineaments on the horizontal gradient of the Bouguer gravity anomaly map (dashed lines bounding DB and KLD, Figure 6a), suggestive of truncations juxtaposing significantly different exposure levels. Late extension may be responsible for differential uplift of blocks (Wodicka *et al*., 2016; Tschirhart *et al*., 2016).

In the Melville region further to the northeast (Area 1 on Figures 1, 2, 3), northeasterly structural, aeromagnetic and gravity trends reflect variable effects of Trans-Hudson deformation and metamorphism (Figures 6a, 6b). Areas dominated by the <1.897 Ga Penhryn Group (Partin *et al*., 2014) and the Repulse Bay block (Laflamme *et al*., 2014) underwent amphibolite to granulite facies metamorphism between 1.84 and 1.82 Ga (Laflamme *et al*., 2017), whereas the Prince Albert block to the north retains Archean fabrics. MT inversions have delineated the subsurface boundary between the Prince Albert block, with thicker lithosphere and moderate resistivity, and the Repulse Bay block, with high resistivity and thinner lithosphere (Spratt *et al*., 2013a). Geological mapping identified the absence of 2.6 Ga Snow Island Suite rocks in the Repulse Bay and Prince Albert blocks and thus suggested accretion to the Rae after 2.6 Ga (Peterson *et al*., this volume). The proposed contact in Peterson *et al*. (this volume) is demarcated by a notable gravity lineament between CBb and RBb

(Figure 6a) and slight break in the mantle resistivity structure in Profile 2 and Profile 3 from Spratt *et al*. (2014).

### *5.3 Metallogenic implications*

One of the most challenging goals of the GEM program has been to understand the distribution of mineral resources and their tectonic controls across the Rae craton. While the protracted orogenic history that affected the Rae craton provided multiple opportunities for reactivation of major crustal structures, only some of these events channelled mineralizing fluids along some structures. Therefore, defining the geophysical attributes of structures that host uranium and gold deposits of the Rae craton has been a significant contribution (e.g. Lawley *et al*., 2015, 2016; Jamison *et al*., 2017; Ma, 2018; Ma *et al*., 2019; Martel *et al*., 2018; Tschirhart *et al*., 2019; 2020; Jefferson *et al*., this volume).

Gold deposits and showings of the Rae craton exhibit the attributes of orogenic gold systems, including spatial association with faults and shear zones (Figure 7; Sherlock *et al*., 2004; Carpenter *et al*., 2005; Davies *et al*., 2010; Pehrsson *et al*., 2013; 2014a; Lawley *et al*., 2015; 2016; Janvier *et al*., 2015). Most deposits - Meadowbank, Meliadine, Three Bluffs, as well as numerous gold showings - occur in volcanic-dominated sequences of Archean age reworked during Paleoproterozoic tectonism (1.9–1.8 Ga). The deposits occur along regional-scale or second-order faults that acted as conduits for mineralizing fluids (Figure 7; Lawley *et al*., 2015). In the Meliadine camp, faults and shear zones likely relate to terrane suturing between the Chesterfield-Rae block and Hearne craton to the south (Pehrsson *et al*., 2014a; Lawley *et al*., 2016). In this largely drift-covered region, interpretation of high-resolution aeromagnetic data has identified additional gold-prospective corridors (Pehrsson *et al*., 2014a) not as evident on the legacy datasets.

Similar concepts of fault reactivation and fluid channelling apply to uranium metallogeny within the Rae craton (Jefferson and Delaney, 2007; Jefferson *et al*., this volume). A recent example of the metallogenic link between basement structure reactivation and uranium is the regional-scale Patterson Lake corridor (PLC) south of the Athabasca Basin. In this region, basement features of the Clearwater Domain (Stern *et al*., 2003), including ductile shear zones, high heat-producing intrusions and basin growth faults, are associated with U mineralization in the overlying Athabasca Basin (Figure 8; Tschirhart *et al*., 2020). Ashton *et al*. (2018) noted that the prominent linear gravity low associated with the Clearwater Domain extends northeastward, and geophysical products presented here demonstrate their continuity into the Baker Lake area, south of the northeastern Thelon Basin (Figure 8) and co-location with the major mineralized faults of the South Rae (Jamison *et al*., 2017, Thiessen *et al*., 2019; McCurdy *et al*., 2016). Both unconformity-style and basement-hosted uranium deposits and occurrences, as well as rare earth element (REE) anomalies (Acosta-Gongora *et al*., 2017) occur along this trend, which parallels the trace of the 1.84–1.81 Ga Baker Lake Group basin depocentres and related magmatism (Peterson *et al*., 2002; Percival *et al*., 2016; Card, 2018). The association between ca 1.85–1.80 Ga intrusions, including alkaline rocks (Card, 2018) and elevated U-Th-REE contents makes Ashton *et al*. (2018)'s suggestion of a potential genetic link between the intrusions and younger U mineralization intriguing.

In the Kiggavik uranium camp (Figures 4, 5, 8), linkages can be made between reactivated basement faults at regional to deposit scales, basin development, hydrothermal fluid flow and uranium occurrences around the northeastern Thelon Basin (Tschirhart *et al*., 2013c; Tschirhart and Pehrsson, 2016; Jefferson *et al*. this volume). These spatial and process linkages were established by integration of geophysical and geological data acquired under the GEM program (Tschirhart *et al*., 2011a).

Given the possible conductive mantle pathways noted by Spratt *et al*. (2014) below Hudson-age intrusions in the Committee Bay and Repulse Bay blocks (Figure 6a), it is notable that Peterson *et al*. (2002) proposed that these suites host mantle melts and major metasomatic components. Significantly, the metasomatizing fluids could provide linkage to the observed low crustal resistivity MT response. Furthermore, Tschirhart *et al*. (2013b) modelled eastern extensions of Hudson magmatism (SLIC) underlying the Kiggavik uranium deposit, again demonstrating the potential for mineralization where 1.8 Ga magmatism, reactivated crustal structures, and basin fluid-reduction processes intersected.

In the TTZ and northeast Thelon regions, Ma (2018) noted that all known uranium occurrences are located at the intersections of, hydrothermally altered, east-northeast and northeast-trending brittle fault systems (including the northeast-trending McDonald fault array) that are localized along earlier ductile shear zones (Tschirhart *et al.*, 2017; Anand and Jefferson, 2017; Hunter *et al.*, 2017). Ma (2018)'s research on the Bathurst fault in the TTZ (Figure 1) documented brittle deformation after 1840 Ma, fluid-rock interaction, and thus enhanced basement permeability. Preliminary age constraints on deposition of sediments in the northeast Thelon Basin are compatible with the temporal constraints on ductile deformation in the Bathurst fault system (*ca.* 1850–1830 Ma; Ma *et al.,* 2019). Overprinting brittle deformation occurred after *ca.* 1810 Ma (Hunter *et al.*, 2018). As the intersection of the Bathurst fault array and MacDonald fault coincides with the Thelon Basin depocentre (Jefferson *et al.*, 2015; Tschirhart *et al.*, 2014, 2017; Tschirhart and Pehrsson, 2016), this establishes significant potential in the basin's underexplored western and northern margins, owing to possible fluid pathways for uranium mineralization along the Bathurst array. This is particularly true along its intersection with additional deep-seated structures such as the McDonald fault and Howard Lake fault zone (Tschirhart and Pehrsson, 2016).

## 6.0 SUMMARY AND OUTSTANDING PROBLEMS

Numerous studies have demonstrated the utility of high-resolution aeromagnetic maps in resolving near-surface features at a range of scales. Regional features such as the Rae craton boundaries—the TTZ and STZ—are evident even at the coarse resolution of regional maps. Much finer resolution is required to follow these boundaries through complexly intruded, deformed and metamorphosed zones. For example, magmatism in the TTZ extended over tens of millions of years, and was accompanied by granulite-facies metamorphism, local basin development, and both ductile and brittle deformation, producing a variety of detailed/complex aeromagnetic features (Berman *et al.*, 2018; Whalen *et al.*, 2018). Conversely, the trajectory of the STZ east of Dubawnt Lake is obscure on regional aeromagnetic maps. High-resolution maps, in concert with detailed geological interpretation, show a complex boundary zone characterized by thrust and transcurrent faults, folds and rock packages of different ages and origins (Pehrsson *et al.,* 2014a; Lawley *et al.*, 2016), yielding no single feature with clear geophysical expression.

Magnetotelluric datasets proved vital for understanding the deep lithospheric structure of the Rae craton and the relationship to surface geological features. For example, when interpreted alongside higher resolution datasets such as aeromagnetic data, key crustal breaks were identified such as the break between the Repulse Bay and Committee Bay blocks. The gravity data further contributed to this enhanced understanding by identifying subsurface density contrasts that demarcated terrain boundaries (e.g. Repulse Bay and Prince Albert blocks in Melville Peninsula) and low density intrusive centres (e.g. 1.85–1.80 Ga Hudson granite suite). While not all features are present in all geophysical datasets, when used in concert they offer the ability to probe the nature of major geological features by visualizing features at a variety of scales and highlighting physical property contrasts related to the metamorphic, structural, geological and alteration histories. Unfortunately, numerous geological models are permitted by the current level of knowledge of the Rae boundaries in the third dimension, based on sparse gravity and MT data sets. This uncertainty regarding the dip and continuity of major crustal features remains an obstacle to broad understanding of tectonic evolution, although the long-lived nature and attendant complexity may preclude tracing these features to mantle depths using existing geophysical methods.

Features related to gold and uranium mineralization are commonly at a finer scale and have been successfully imaged geophysically by modern data in concert with geological models. For example, uranium metallogenic models view reactivated faults in the basement beneath Proterozoic sedimentary basins as channels for mineralizing fluids (Jefferson and Delaney, 2007; Potter *et al.*, 2020). Geophysical models of the sub-Thelon basement show the distribution of key features including reactivated structures and intrusive units with potential linkage to uranium mineralization processes (Tschirhart *et al.*, 2013b; 2013c; 2014; Tschirhart and Pehrsson, 2016, Potter *et al.*, 2020). Exploration of the basal units of thick, flat-lying sedimentary basins remains a challenging enterprise. Derivative products on modern aeromagnetic datasets (e.g. Figure 7) clearly delineate structural breaks related to gold mineralization in the Chesterfield Inlet region emphasizing the importance of updating the aeromagnetic survey coverage in prospective terrains.

**Acknowledgements**

This contribution was produced as part of the Geo-mapping for Energy and Minerals Program and on-going research in the Uranium activity of the Targeted Geoscience Initiative Program. Brad Harvey is thanked for his technical support. Discussions with Jeremy Powell and Eric Potter provided appreciated insight. Comments and reviews from Nathan Hayward and Richard Smith improved the quality of the manuscript. This is Geological Survey of Canada contribution 2020XXXX.



**References**

Acosta-Góngora, P., Pehrsson, S.J., Martel, E., Lauzon, G., Jamison, D., 2017. South Rae Project: preliminary field observations (2015) and lake sediment analysis, Northwest Territories and Saskatchewan; Geological Survey of Canada, Scientific Presentation 67, 2017, 47 pages, https://doi.org/10.4095/302765

Acosta-Góngora, P., Pehrsson, S.J., Sandeman, H.A., Martel, E., Peterson, T.D., 2018. The Ferguson Lake deposit: an example of Ni-Cu-Co-PGE mineralization emplaced in a back-arc basin setting? Canadian Journal of Earth Sciences 55, 958–979.

Anand, A. and Jefferson, C.W., 2017. Outcropping and remotely predicted lineaments, faults, fractures and dykes in the Kiggavik uranium camp of Nunavut; Geological Survey of Canada, Open File 7896, 1 sheet.

Ashton, K., Card, C. and Rayner, N., 2018. A new U-Pb age for the Hudson granites and lamprophyre dykes in the southern Rae Province of Saskatchewan; Summary of Investigations 2018, Volume 2, Saskatchewan Geological Survey, Saskatchewan Ministry of Energy and Resources, Miscellaneous Report 2018-4.2, Paper A-6, 15 p. and 2 appendices

Berman, R.G., 2010. Metamorphic map of the western Churchill Province. Open File 5279, Geological Survey Canada, Canada

Berman, R.G., Sanborn-Barrie, M., Stern, R.A., and Carson, C.J., 2005. Tectono- metamorphism at *ca.* 2.35 and 1.85 Ga in the Rae domain, western Churchill Province, Nunavut, Canada: insights from structural, metamorphic and in situ geochronological analysis of the southwestern Committee Bay belt; Canadian Mineralogist, 43, 409–442. doi:10.2113/gscanmin.43.1.409

Berman, R., Davis, W., and Pehrsson, S., 2007. Collisional Snowbird tectonic zone resurrected: Growth of Laurentia during the 1.9 Ga accretionary phase of the Hudsonian orogeny; Geology, 35, 911-914.

Berman, R.G., Rayner, N., Sanborn-Barrie, M., and Chakungal, J., 2011. New constraints on the tectonothermal history of Southampton Island, Nunavut, provided by in situ SHRIMP geochronology and thermobarometry; Geological Survey of Canada, Current Research 2011-6, 14 p. doi:10.4095/287287

Berman, R.G., Pehrsson, S., Davis, W.J., Ryan, J.J., Qui, H. and Ashton, K.E., 2013a. The Arrowsmith orogeny: Geochronological and thermobarometric constraints on its extent and tectonic setting in the Rae craton, with implications for pre-Nuna supercontinent reconstruction. Precambrian Research, 232, 44-69.

Berman, R.G., Sanborn-Barrie, M., Rayner, N. and Whalen, J., 2013b. The tectonometamorphic evolution of Southampton Island, Nunavut: Insight from petrologic modeling and in situ SHRIMP geochronology of multiple episodes of monazite growth; Precambrian Research, 232, 140-166.

Berman, R.G., Davis, W.J., Corrigan, D. and Nadeau, L., 2015. Insights into the tectonothermal history of Melville Peninsula, Nunavut, provided by in situ SHRIMP geochronology and thermobarometry. Geological Survey of Canada, Current Research 2015-4, 22 p. https://doi.org/10.4095/295852

Berman, R.G., Sanborn-Barrie, M., Nadeau, L., Brouillette, P., Camacho, A., Davis, W.J., McCurdy, M.W., McMartin, I., Weller, O.M., Chadwick, T., Liikane, D.A., and Ma, S., 2016. Report of activities for the geology and mineral potential of the Chantrey-Thelon area: GEM-2 Rae project; GSC Open File, v. 8129, 12 p. doi:10.4095/299386

Berman, R.G., Davis, W.J., Sanborn-Barrie, M., Whalen, J.B., Taylor, B.E., McMartin, I., McCurdy, M.W., Mitchell, R.K., Ma, S., Coyle, M., Roberts, B. and Craven, J.A., 2018. Report of activities for the GEM-2 Chantrey-Thelon activity: Thelon Tectonic Zone project, Nunavut. Geological Survey of Canada, Open File 8372, 19 p. https://doi.org/10.4095/306622

Blakely, R.J. and Simpson, R. W., 1986. Approximating edges of source bodies from magnetic or gravity anomalies; Geophysics, 51, 1494-1498.

Buchan, K.L. and Ernst R.E., 2020. Paleoproterozoic dyke swarms and large igneous provinces of northern Canada and their use in understanding extension, rifting and paleocontinental Reconstructions. In Canada’s Northern Shield: new perspectives from the Geomapping for Energy and Minerals Program. Edited by Pehrsson, S.J., Wodicka, N., and Percival, J.   GSC Bulletin XXX, pp xx-xx.

Calhoun, L., White, J.C., Jefferson, C.W., Patterson, J., and Tschirhart, V., 2014. Integrated geodatabase study of the complexly deformed U-hosting Paleoproterozoic Amer Group, Nunavut; Geological Survey of Canada, Scientific Presentation 19, 1 ppt file. https://doi.org/10.4095/293108.

Card, C.D., 2018. The Patterson Lake alkaline igneous complex: Evidence for deep-seated structural control in the Patterson Lake corridor, and implications for mineral exploration. Summary of Investigations 2018, Volume 2, Saskatchewan Geological Survey, Saskatchewan Ministry of Energy and Resources, Miscellaneous Report 2018-4.2, Paper A-9, 19p.

Card, C.D., Bosman, S.A., Slimmon, W.L., Delaney, G., Heath, P., Gouthas, G. and Fairclough, M., 2010. Enhanced Geophysical Images and Multi-scale Edge (Worm) Analysis for the Athabasca Region; Geological Survey of Saskatchewan, Open File 2010-46.

Carpenter, R.L., Duke, N.A., 2004. Geological setting of the West Meliadine gold deposits, Western Churchill Province, Nunavut, Canada. Explor. Min. Geol. 13, 49–65.

Carpenter, R.L., Duke, N.A., Sandeman, H.S., Stern, R., 2005. Relative and absolute timing of gold mineralization along the Meliadine Trend, Nunavut, Canada: evidence for Paleoproterozoic gold hosted in an Archean greenstone belt. Econ. Geol. 100, 567–576.

Chacko, T., De, S.K., Creaser, R.A., and Muehlenbachs, K., 2000. Tectonic setting of the Taltson Magmatic zone at 1.9 to 2.0 Ga: a granitoid-based perspective; Canadian Journal of Earth Sciences, 37, 1597–1609.

Cook, F.A., Percival, J.A. and Clowes, R.M., 2012. Tectonic styles in Canada: LITHOPROBE perspectives on the evolution of the North American continent; in Tectonic Styles in Canada: the LITHOPROBE Perspective; Percival, J A (ed.); Cook, F A (ed.); Clowes, R M (ed.); Geological Association of Canada, Special Paper no. 49, p. 467-498.

Corrigan, D., Pehrsson, S., Wodicka, N., De Kemp, E., 2009. The Palaeoproterozoic Trans-Hudson Orogen: a prototype of modern accretionary processes. In: Murphy, J.B., Keppie, J.D., Hynes, A.J. (Eds.), Ancient Orogens and Modern Analogues. Geological Society, London, Special Publications, 327, 457–479.

Corrigan, D., Nadeau, L., Brouillette, P., Wodicka, N., Houlé, M.G., Tremblay, T., Machado, G., and Keating, P., 2013. Overview of the GEM Multiple Metals — Melville Peninsula project, central Melville Peninsula, Nunavut; Geological Survey of Canada, Current Research 2013-19, 17 p. doi:10.4095/292862

Davies, T., Richards, J.P., Creaser, R.A., Heaman, L.M., Chacko, T., Simonetti, A., Williamson, J., and McDonald, D.W., 2010. Paleoproterozoic age relationships in the Three Bluffs Archean iron formation-hosted gold deposit, Committee Bay Greenstone Belt, Nunavut, Canada. Exploration and Mining Geology 19, 55–80.

Davis, W.J., Hanmer, S. and Sandeman, H.A., 2004. Temporal evolution of the Neoarchean Central Hearne supracrustal belt: rapid generation of juvenile crust in a suprasubduction zone setting. Precambrian Research, 134, 85-112.

Davis, W.J., Hanmer, S., Tella, S., Sandeman, H.A., and Ryan, J.J., 2006. U–Pb geochronology of the MacQuoid supracrustal belt and Cross Bay plutonic complex: key components of the northwestern Hearne subdomain, western Churchill Province, Nunavut, Canada. Precambrian Research, 145, 53–80.

Davidson, G.I. and Gandhi, S.S. 1989. Unconformity-related U-Au mineralization in the Middle Proterozoic Thelon sandstone, Boomerang Lake prospect, Northwest Territories, Canada. Economic Geology, 84, 143-157.

Dubé, B., Mercier-Langevin, P., Castonguay, S., McNicoll, V.J., Bleeker, W., Lawley, C.J.M. De Souza, S., Jackson, S.E., Dupuis, C., Gao, J-F; Bécu, V., Pilote, P., Goutier, J., Beakhouse, G.P., Yergeau, D., Oswald, W., Janvier, V., Fontaine, A., Pelletier, M., Beauchamp, A-M., Malo, M., Katz, L.R., Kontak, D.J., Tóth, Z., Lafrance, B., Gourcerol, B., Thurston, P.C., Creaser, R.A., Enkin, R.J., El Goumi, N., Grunsky, E.C., Schneider, D.A., Kelly, C.J. and Lauzière, K., 2015. Precambrian lode gold deposits - a summary of TGI-4 contributions to the understanding of lode gold deposits, with an emphasis on implications for exploration; in Targeted Geoscience Initiative 4: Contributions to the understanding of Precambrian lode gold deposits and implications for exploration; Dubé, B (ed.); Mercier-Langevin, P (ed.); Geological Survey of Canada, Open File 7852, 2015 p. 1-24, https://doi.org/10.4095/296625

Dziawa, C., Gaidies, F. and Percival, J., 2019. Conditions and timing of low-pressure – high-temperature metamorphism in the Montresor Belt, Rae Province, Nunavut. Canadian Journal of Earth Sciences, 56, 654-671, doi.org/10.1139/cjes-2018-0184.

Enkin, R.J., Corriveau, L., and Hayward, N., 2016. Metasomatic alteration control of physical properties in the Great Bear magmatic zone (Northwest Territories, Canada). Economic Geology, 111, 2073-2085.

Enkin, R.J., 2018. Canadian rock physical property database: first public release. Geological Survey of Canada, Open File 8460, 1 .zip file. https://doi.org/10.4095/313389

Gibb, R.A. and Thomas, M.D., 1977. The Thelon front: A cryptic suture in the Canadian shield? Tectonophysics, 38, 211-222.

Gilligan, A., Bastow, I.D. and Darbyshire, F.A., 2016. Seismological structure of the 1.8 Ga Trans-Hudson Orogen of North Americ*a.* Geochemistry, Geophysics, Geosystems. 17, 2421–2433. doi:10.1002/2016GC006419.

Goldfarb, R.J., Baker, T., Dubé, B., Groves, D.I., Hart, C.J.R. and Gosselin, P., 2005. Distribution, character, and genesis of gold deposits in metamorphic terranes; in One hundredth anniversary volume 1905 - 2005; Hedenquist, J W (ed.); Thompson, J F H (ed.); Goldfarb, R J (ed.); Richards, J P (ed.); Economic geology and the bulletin of the Society of Economic Geologists 2005 p. 407-450, https://doi.org/10.2113/gsecongeo.98.1.1

Gordon, T.M. and Heywood, W.W., 1987. Geology, Daly Bay. Geological Survey of Canada Map 1652A.

Gordon, T.M., and Lawton, D.C., 1995. Geometry of the allochthonous Daly Bay Complex, Northwest Territories: a model constrained by geology and a three-dimensional gravity interpretation. Canadian Journal of Earth Sciences, 32, 1292-1302.

Hadlari, T., Rainbird, R.H., 2011. Retro-arc extension and continental rifting: a model for the Paleoproterozoic Baker Lake Basin, Nunavut. Canadian Journal of Earth Sciences 48, 1232-1258, https://doi.org/10.1139/E11-002

Hanmer, S., Williams, M. and Kopf, C., 1995. Striding-Athabasca mylonite zone: implications for the Archean and Early Proterozoic tectonics of the western Canadian Shield. Canadian Journal of Earth Sciences, 32, 178-196.

Hanmer, S., Sandeman, H.A., Davis, W.J., Aspler, L.B., Rainbird, R.H., Ryan, J.J., Relf, C. and Peterson, T., 2004. Geology and Neoarchean tectonic setting of the Central Hearne supracrustal belt, Western Churchill Province, Nunavut, Canada. Precambrian Research, 134, 63-83.

Harris, J.R., Hillary, E.M., Percival, J A; Buller, G; Buenviaje, R; Bazor, D; Baer, S; Kiessling, G M; Pehrsson, S J; Davis, W; Berman, R G; Wodicka, N; Beauchemin, M; Coyne, M; Therriault, A M., 2013. Geo-mapping Frontiers: Updated information on the regions covered by Operations Baker, Bathurst, Keewatin, Northern Keewatin, Thelon and Wager; Nunavut and Northwest Territories. Geological Survey of Canada, Open Files 7434-7448.

Hayward, N., Harris, J.R., Grunsky, E., Beauchemin, M., Jefferson, C., and Peterson, T., 2013. Geo-mapping Frontiers: Predictive Geology Map of the Ennadai Region, Nunavut. Geological Survey of Canada, Open File 7485, 21 p. doi:10.4095/293261

Helmstaedt, H.H. and Pehrsson, S.J., 2012. Geology and tectonic evolution of the Slave Province – A post Lithoprobe perspective. Chapter 7 in Tectonic Styles in Canada: The Lithoprobe Perspective. Edited by J.A. Percival, F.A. Cook and R.M. Clowes. Geological Association of Canada, Special Paper 49, 379-466.

Hoffman, P., 1988. United plates of America, the birth of a craton: early Proterozoic assembly and growth of Laurentia. Annual Review of Earth and Planetary Sciences, 16, 543-603.

Hunter, R., Lafrance, B., Lesperance, J., and Zaluski, G. 2012. The Qavvik-Tatiggaq Trend: an evolving unconformity-related uranium corridor of the northeast Thelon Basin, Nunavut (abstract) In: GAC-MAC Annual Meeting, St. John's, Abstracts, v. 35, 60.

Hunter, R.C., Lafrance, B., Heaman, L.M., Zaluski, G., and Thomas, D. 2018. Geology, lithogeochemistry and new LA-ICP-MS U-Pb geochronology of the Aberdeen Lake area, Nunavut: new insights into the Neoarchean tectonic evolution of the central Rae Domain. Precambrian Research, 310, 114-132.

Jamison, D., 2018. Deformation history of the Black Bay Fault, Northwest Territories. M.Sc. Thesis, University of Waterloo, 133 pages.

Jamison, D., Acosta-Góngora, P., Knox, B.K., Pehrsson, S.J., and Lin, S., 2017. Deformation history of the Black Bay Fault and associated mineralization, Northwest Territories. Geological Survey of Canada, Scientific Presentation 69, 1 sheet. https://doi.org/10.4095/304197

Janvier, V., Castonguay, S., Mercier-Langevin, P., Dubé, B., Malo, M., McNicoll, V.J., Creaser, R.A., de Chavigny, B. and Pehrsson, S.J., 2015. Geology of the banded iron formation-hosted Meadowbank gold deposit, Churchill Province, Nunavut; in Targeted Geoscience Initiative 4: Contributions to the understanding of Precambrian lode gold deposits and implications for exploration; Dubé, B. (ed.); Mercier-Langevin, P. (ed.); Geological Survey of Canada, Open File 7852, p. 255-269, https://doi.org/10.4095/296646

Jefferson, C.W. and Delaney, G., 2007. EXTECH IV: Geology and Uranium EXploration TECHnology of the Proterozoic Athabasca Basin, Saskatchewan and Alberta. Geological Survey of Canada, Bulletin 588, 645 p; 1 CD-ROM, https://doi.org/10.4095/223742

Jefferson, C.W., Hunter, R., McLaren, M., Peterson, T., Skulski, T., Rainbird, R., Young, G.M., Gandhi, S.S., Costello, K., 2011. Northeastern Thelon Basin Uranium Region: Geological compilation for geophysical consortium planning. Geological Survey of Canada, Open File 6950, 2011, 1 sheet, https://doi.org/10.4095/288801

Jefferson, C.W., White, J.C., Young, G.M., Patterson, J., Tschirhart, V., Pehrsson, S.J., Calhoun, L., Rainbird, R.H., Peterson, T.D., Davis, W.J.. Tella, S., Chorlton, L.B., Scott, J.M.J., Percival, J.A., Morris, W.A., Keating, P., Anand, A., Shelat, Y. and MacIsaac, D., 2015. Outcrop and remote predictive geology of the Amer Belt and basement beside and beneath the northeast Thelon Basin, in parts of NTS 66-A, B, C, F, G and H, Kivalliq Region, Nunavut. Geological Survey of Canada, Open File 7242, 1 sheet.

Jefferson, C.W., Pehrsson, S., Tschirhart, V., Peterson, T., Chorlton, L., Bethune, K., Davis, W., McNicoll, V., Paulen, R.C. and Rayner, N., 2021. Geology and metallogeny of the northea st Thelon Basin region and comparison with the Athabasca Basin. this volume, xx-xx.

Jobin, D.M., Veronneau, M. and Miles, W., 2017. Isostatic residual gravity anomaly map, Canada. Geological Survey of Canada, Open File 8076, scale 1:7 500 000.

Jones, A.G., Snyder, D., Hanmer, S., Asudeh, I. and White, D., 2002. Magnetotelluric and teleseismic study across the Snowbird Tectonic Zone: A Neoarchean mantle suture? Geophysical Research Letters, 29, 10-1-10-4.

Kellett, D.A., Pehrsson, S., Skipton, D.R., Regis, D., Camacho, A., Schneider, D.A. and Berman, R., 2020. Thermochronological history of the northern Canadian Shield. Precambrian Research, 342, https://doi.org/10.1016/j.precamres.2020.105703.

Kiss, F. and Tschirhart, V., 2017, Aeromagnetic survey of the Marguerite River area, Saskatchewan. Geological Survey of Canada, Open Files 8259-8273.

Lawley, C.J.M., Creaser, R.A., Jackson, S.E., Yang, Z., Davis, B.J., Pehrsson, S.J., Dube, B., Mercier-Langevin, P., and Daillancourt, D., 2015. Unraveling the Western Churchill Province Paleoproterozoic gold metallotect: Constraints from Re-Os arsenopyrite and U-Pb xenotime geochronology and LA-ICP-MS arsenopyrite trace element chemistry at the BIF-hosted Meliadine gold district, Nunavut, Canada. Economic Geology, 110, 1425-1454

Lawley, C.J.M., McNicoll, V., Sandeman, H., Pehrsson, Simard, M., Castonguay, S., Mercier-Langevin, P., Dubé, B., 2016. Age and geological setting of the Rankin Inlet greenstone belt and its relationship to the gold endowment of the Meliadine gold district Nunavut, Canad. Precambrian Research, 275, 471-495.

LaFlamme, C., McFarlane, C.R.M., Corrigan, D. and Wodicka, N., 2014. Origin and tectonometamorphic history of the Replusle Bay block, Melville Peninsula, Nunavut: exotic terrane or deeper level of the Rae craton? Canadian Journal of Earth Sciences, 51 , 1097-1122.

LaFlamme, C., McFarlane, C.R.M., Fisher, C.M. and Kirkland, C.L., 2017. Multi-mineral geochronology: insights into crustal behaviour during exhumation of an orogenic root. Contributions to Mineralogy and Petrology, 172:9 https://doi.org/10.1007/s00410-017-1331-7.

Liddell, M.V., Bastow, I., Rawlinson, N., Darbyshire, F., Gilligan, A. and Watson, E., 2018. Precambrian plate tectonics in northern Hudson Bay: Evidence from P and S wave seismic tomography and analysis of source side effects in relative arrival-time data sets. Journal of Geophysical Research: Solid Earth, 123, 5690-5709.

Liu, J., Riches, A.J.V., Pearson, D.G., Luo, Y, Kienlen, B., Kjarsgaard, B.A., Stachel, T. and Armstrong, J.P., 2016. Age and evolution of the deep continental root beneath the central Rae craton, northern Canada. Precambrian Research 272, 168-184.

Ma, S., 2018. Structural style and timing and deformation on the Bathurst fault in the eastern Slave craton, western Nunavut, Canada. MSc. Thesis, Queen's University.

Ma, S.M., Kellett, D.A., Godin, L., and Jercinovic, M.J., 2019. Localization of the brittle Bathurst fault on pre-existing fabrics: A case for structural inheritance in the northeastern Slave craton, western Nunavut, Canada. Canadian Journal of Earth Sciences, https://doi.org/10.1139/cjes-2019-0100

Mahan, K.H. and Williams, M.L., 2005. Reconstruction of a large deep-crustal terrane: implications for the Snowbird tectonic zone and early growth of Laurentia. Geology, 33, 385-388.

Martel, E., Pehrsson, S.J., Percival, J., Acosta-Góngora, P., Thiessen, E., Regis, D., Jamieson, D., Neil, B., and Knox, B., 2018. Geology and mineral potential of the southern Rae Craton, Northwest Territories, NTS 75-G and H. Geological Survey of Canada, Open File 8194, 1 poster. https://doi.org/10.4095/306542

Martel, E., 2021…..this volume

McCurdy, M.W., Berman, R.G., Kerr, D.E. and Vaive, J.E., 2013. Geochemical, mineralogical and kimberlite indicator mineral data for silts, heavy mineral concentrates and waters, Duggan Lake area, Nunavut (NTS 76-H and 76-I South). Geological Survey of Canada, Open File 7471, 22 p, doi: 10.4095/293044.

McCurdy, M.W., Pehrsson, S.J., Falck, H., Day, S.J.A., and Campbell, J.E., 2016. Geochemical data for lake sediments and surface waters, Abitau Lake area, Northwest Territories (NTS 75-B); Geological Survey of Canada, Open File 8082, 2016, 19 pages, https://doi.org/10.4095/299389

McMartin, I., Randour, I., and Wodicka, N., 2019. Till composition across the Keewatin Ice Divide in the Tehery-Wager GEM-2 Rae project area, Nunavut. Geological Survey of Canada, Open File 8563, 1 .zip file. https://doi.org/10.4095/314707

Mills, A., Berman, R.G., Davis, W.J., Tella, S., Carr, S.D., Roddick, C., and Hanmer, S., 2007. Thermobarometry and geochronology of the Uvauk Complex: a polymetamorphic Neoarchean and Paleoproterozoic segment of the Snow- bird tectonic zone, Nunavut, Canada. Canadian Journal of Earth Sciences, 44, 245–266.

Mowbray, B. and Pehrsson, S.J., 2019. Geochemistry, petrology, and aeromagnetic mapping of the Orpheus dykes, South Rae craton, Northwest Territories. Geological Survey of Canada, Open File 8340, 28 p. https://doi.org/10.4095/311306

Overton, A., 1979. Seismic reconnaissance survey of the Dubawnt Group, districts of Keewatin and Mackenzie. Geological Survey of Canada, Current Research, Part B, Paper 79-1B, pp. 397-400.
Patterson, J.G. 1986. The Amer Belt: remnant of an Aphebian foreland fold and thrust belt. Canadian Journal of Earth Sciences, 23, 2012-2023.

Partin, C.A., Bekker, A., Corrigan, D., Modeland, S., Francis, D., and Davis, D.W., 2014. Sedimentological and geochemical basin analysis of the Paleoproterozoic Penrhyn and Piling groups of Arctic Canada. Precambrian Research, 251, 80-101.

Pehrsson, S.J., Berman, R.G. and Davis, W.J., 2013. Paleoproterozoic orogenesis during Nuna aggregation: A case study of reworking of the Rae craton, Woodburn Lake, Nunavut. Precambrian Research, 232, 167-188.

Pehrsson, S.J., Coyle, M., and Berman, R., 2014a. The GEM Chesterfield gold project: understanding controls on western Churchill gold endowment from the bottom up. Geological Survey of Canada, Open File 7490, 31 p. doi:10.4095/293763

Pehrsson, S.J., Currie, M., Ashton, K.E., Harper, C.T., Paul, D., Pana, D., Berman, R.G., Bostock, H., Corkery, T., Jefferson, C.W., and Tella, S., 2014b. Bedrock geology compilation south Rae and western Hearne provinces, Churchill Province, Northwest Territories, Saskatchewan, Nunavut, Manitoba, and Alberta. Geological Survey of Canada, Open File 5744, scale 1:550 000. doi:10.4095/292232

Pehrsson, S.J., Campbell, J.E., Martel, E., McCurdy, M.W., Agosta-Gongora, P., Theissen, E., Jamieson, D., Lauzon, G., Buller, G., Falck, H., and Dyke, A.S., 2015. Report of 2015 Activities for the Geologic and Metallogenic Framework of the South Rae Craton, Southeast Northwest Territories: GEM 2 South Rae Quaternary and Bedrock Project. Geological Survey of Canada, Open File 7958, 24 p. doi:10.4095/297387.

Pehrsson, S., Berman, R., Percival, J., Regis, D., Wodicka, N., Corrigan, D., 2021. Paleoproterozoic architecture of the northern Canadian Shield. In Canada's Northern Shield: new perspectives from the Geomapping for Energy and Minerals Program. Edited by Pehrsson, S.J., Wodicka, N., and Percival, J. GSC Bulletin XXX, pp xx-xx, this volume

Percival, J.A. and Tschirhart, V., 2017. Trans-Hudsonian far-field deformation effects in the Rae foreland: an integrated geological-3D magnetic model. Tectonophysics, 699, 82-92.

Percival, J.A., Tschirhart, V., Ford, A., and Dziawa, C., 2015. Report of field activities for the geology and mineral potential of the Chantrey-Thelon Area: GEM-2 Montresor Project. Geological Survey of Canada, Open File 7707.

Percival, J.A., Martel, E., Pehrsson, S.J., Acosta-Gongora, P., Regis, D., Thiessen, E., Jamison, D., Neil, B., and Knox, B., 2016. Report of 2016 Bedrock Activities for the Geologic and Metallogenic Framework of the South Rae Craton, Southeast NWT: GEM 2 South Rae Quaternary and Bedrock Project. Geological Survey of Canada, Open File 8142. 17 p. doi:10.4095/299469

Percival, J.A., Davis, W.J., and Hamilton M.A., 2017. U-Pb zircon geochronology and depositional history of the Montresor group, Rae Province, Nunavut, Canada. Canadian Journal of Earth Sciences, 2017, 54, 512-528. https://doi.org/10.1139/cjes-2016-0170

Peterson, T.D., Van Breeman, O., Sandeman, H. and Cousens, B., 2002. Proterozoic (1.85-1.75 Ga) igneous suites of the Western Churchill Province: granitoid and ultrapotassic magmatism in a reworked Archean hinterland; Precambrian Research, 119, 73-100.

Peterson, T.D., Pehrsson, S.J., Skulski, T. and Sandeman, H., 2010. Compilation of Sm=Nd isotope analyses of igneous suites, western Churchill Province. Geological Survey of Canada, Open File 6439, 18 pages. doi:10.4095/285360

Peterson, T.D., Jefferson, C.W., and Anand, A., 2015a. Geological setting and geochemistry of the *ca.* 2.6 Ga Snow Island Suite in the central Rae Domain of the Western Churchill Province, Nunavut; Geological Survey of Canada, Open File 7841, 1 .zip file. doi:10.4095/296599

Peterson, T.D, Scott, J.M.J., LeCheminant, A.N., Tschirhart, V.L., Chorlton, L.B., Davis, W.J., and Hamilton, M.A., 2015b. Nueltin granites and mafic rocks in the Tebesjuak Lake map area, Nunavut: new geochronological, petrological, and geophysical data; Geological Survey of Canada, Current Research 2015-5, 19 p. doi:10.4095/296163

Peterson, T.D., Scott, J.M.J., LeCheminant, A.N., Jefferson, C.W., and Pehrsson, S.J., 2015c. The Kivalliq Igneous Suite: Anorogenic bimodal magmatism at 1.75 Ga in the western Churchill Province, Canada. Precambrian Research, 262, 101-119.

Peterson, T.D., Wodicka, N., Pehrsson, S.J., Acosta-Góngora, P., Tschirhart, V., Jefferson, C.J., Steenkamp, H., Martel, E., Percival, J., and Corrigan, D., 2020. The Rae Province at 2.6 Ga: a Sanukitoid storm on the Canadian Shield. This volume.

Pilkington, M., Miles, W., Ross, G., and Roest, W.R., 2000. Potential-field signatures of buried Precambrian basement in the Western Canada Sedimentary Basin; Canadian Journal of Earth Sciences, 37, 1453-1471.

Potter, E.G., Tschirhart, V. Powell, J.W., Kelly, C.J., Rabiei, M., Johnstone, D., Pehrsson, S., Mount, S., Chi, G., and Bethune, K.M., in press. Formation of unconformity-related uranium deposits: insights from integrated multidisciplinary studies of the Patterson Lake Corridor, northern Saskatchewan. Geological Survey of Canada, Bulletin 615.

Rainbird, R.H., Hadlari, T., Aspler, L.B., Donaldson, J.A., LeCheminant, A.N., and Peterson, T.D., 2003. Sequence stratigraphy and evolution of the paleoproterozoic intracontinental Baker Lake and Thelon basins, western Churchill Province, Nunavut, Canada; Precambrian Research, 125, 21-53.
Rainbird, R.H., Davis, W.J., Pehrsson, S., Wodicka, N., Rayner, N., and Skulski, T., 2010. Early Paleoproterozoic supracrustal assemblages of the Rae domain, Nunavut, Canada: intracratonic basin development during supercontinent break-up and assembly; Precambrian Research, 181, 167–186.

Ramaekers, P., Jefferson, C.W., Yeo, G.M., Collier, B., Long, D.G.F., Drever, G., McHardy, S., Jiricka, D., Cutts, C., Wheatley, K., Catuneanu, O., Bernier, S., Kupsch, B., and Post, R.T., 2007. Revised geological map and stratigraphy of the Athabasca group, Saskatchewan and Alberta; Bulletin of the Geological Survey of Canada, 588, 155–191.

Regis, D., Martel, E., Davis, W.J., Pehrsson, S.J., 2017. U-Pb zircon geochronology of metaplutonic rocks across the southern Rae province, Northwest Territories; Geological Survey of Canada, Open File 8254, 1 .zip file. https://doi.org/10.4095/302772

Regis, D., Davis, W.J., Ryan, J.J., Berman, R.G., Pehrsson, S., Joyce, N.L. and Sandeman, H.A. 2019. Multiple burial–exhumation episodes revealed by accessory phases in high-pressure granulite-facies rocks (Rae craton, Nunavut, Canada). Contributions to Mineralogy and Petrology 174: 41.

Regis, D., Pehrsson, S.J., Martel, E., Thiessen E., Peterson, T. and Kellett, D., 2021. Post-1.9 Ga evolution of the south Rae craton (Northwest Territories, Canada): A Paleoproterozoic orogenic collapse system. Precambrian Research, 355, 106105.

Roberts, B., Craven, J.A., Berman, R.G., and Roots, E., 2015. Preliminary results of a Magnetotelluric survey in the Chantrey-Thelon area; GEM-2 Thelon tectonic zone project; Geological Survey of Canada, Open File 7931, 29 p. doi:10.4095/297426

Ross, G.M., 2002. Evolution of Precambrian continental lithosphere in Western Canada: results from Lithoprobe studies in Alberta and beyond. Canadian Journal of Earth Sciences, 39, 413-437.

Sanborn-Barrie, M., Carr, S.D., and Theriault, R., 2001. Geochronological constraints on metamorphism, magmatism and exhumation of deep-crustal rocks of the Kramanituar Complex, with implications for the Paleoproterozoic evolution of the Archean western Churchill Province, Canada; Contributions to Mineralogy and Petrology, 141, 592-612.

Sanborn-Barrie, M., Davis, W.J., Berman, R.G., Rayner, N., Skulski, T., and Sandeman, H., 2014a. Neoarchean continental crust formation and Paleoproterozoic deformation of the central Rae craton, Committee Bay belt, Nunavut; Canadian Journal of Earth Sciences, 51, 635-667.

Sanborn-Barrie, M., Chakungal, J., James, D.T., Rayner, N., and Whalen, J.B., 2014b. Precambrian bedrock geology, Southampton Island, Nunavut; Geological Survey of Canada, Canadian Geoscience Map 132, scale 1:250 000. doi:10.4095/293328

Sanborn-Barrie, M., Regis, D., Ford, A., Osinchuk, A., and Drayson, D., 2018. Report of activities for the GEM-2 Boothia Peninsula–Somerset Island Project: integrated geoscience of the Northwest Passage, Nunavut; Geological Survey of Canada, Open File 8339, 16 p. https://doi.org/10.4095/306597

Sanborn-Barrie, M., Regis, D., Ford, A., 2019a. Integrated Geoscience of the Northwest Passage, Nunavut; GEM-2 Boothia Peninsula-Somerset Island Project, report of activities 2018; Geological Survey of Canada, Open File 8557, 17 p. https://doi.org/10.4095/314501

Sanborn-Barrie, M., Camacho, A. and Berman, R., 2019b. High-pressure, ultrahigh-temperature 1.9 Ga metamorphism of the Kramanitaur Complex, Snowbird Tectonic Zone, Rae Craton; Contributions to Mineralogy and Petrology, 174 (14), 26 p.

Sherlock, R., Pehrsson, S., Logan, A.V., Hrabi, R.B., Davis, W.J., 2004. Geological setting of the Meadowbank gold deposits, Woodburn Lake Group, Nunavut. Exploration and Mining Geology, 13, 67–107.

Sandeman, H.A., Davis, W.J., Hanmer, S., Tella, S., Ryan, J.J., 2006. Tectonic evolution of the northwestern Hearne domain, western Churchill Province, Canada: a petrochemical perspective from the MacQuoid supracrustal belt. Precambrian Research, 144, 140–165.

Schultz, M., Chacko, T., Heaman, L.M., Sandeman, H., Simonetti, A., and Creaser, R.A., 2007. The Queen Maud Block: a newly recognized Paleoproterozoic (2.4–2.5 Ga) terrane in northwest Laurentia; Geology, 35, 707–710.

Skulski, T., Spratt, J.E., Craven, J.A., Jones, A.G., and Snyder, D.B. 2014. Deep crustal structure of the Rae Craton, mainland Nunavut. In Annual Meeting of the Geological Association of Canada. Mineralogical Association of Canada, Fredericton, N.B., 2014.

Skulski, T., Paul, D., Sandeman, H., Berman, R.G., Chorlton, L., Pehrsson, S.J., Rainbird, R.H., Davis, W.J., and Sanborn-Barrie, M., 2018. Bedrock geology, central Rae Craton and eastern Queen Maud Block, western Churchill Province, Nunavut; Geological Survey of Canada, Canadian Geoscience Map 307, scale 1:550 000. https://doi.org/10.4095/308348

Snyder, D.B., Berman, R.G., Kendall, J.-M., and Sanborn-Barrie, M., 2013. Seismic anisotropy and mantle structure of the Rae craton, central Canada, from joint interpretation of SKS splitting and receiver functions. Precambrian Research, 232, 189-208.

Snyder, D.B., Craven, J.A., Pilkington, M., Hillier, M.J., 2015. The three-dimensional construction of the Rae craton, central Canada. Geochemistry, Geophysics, Geosystems, 16, 3555-3574. http://dx.doi.org/10.1002/2015GC005957.

Spratt, J.E., Snyder, D.B. and Craven, J.A., 2011. A magnetotelluric survey across the Committee Bay belt and Rae craton in the Churchill province of Nunavut; Geological Survey of Canada, Open File 6825, 28 p.

Spratt, J.E., Snyder, D.B. and Craven, J.A., 2012a. Magnetotelluric soundings in the Committee Bay Belt, northern Churchill area, Nunavut; Geological Survey of Canada, Open File 7063, 37 p. doi:10.4095/289836

Spratt, J.E., Craven, J.A., and Sanborn-Barrie, M., 2012b. Southampton Island magnetotelluric survey: data acquisition and preliminary analysis; Geological Survey of Canada, Open File 6988, 39 p. doi:10.4095/291384

Spratt, J., Jones, A.G., Corrigan, D., and Hogg, C., 2013a. Lithospheric geometry revealed by deep-probing magnetotelluric surveying, Melville Peninsula, Nunavut; Geological Survey of Canada, Current Research 2013-12, 14 p. doi:10.4095/292482

Spratt, J. E., Roberts, B., Kiyan, D. and Jones, A.G., 2013b. Magnetotelluric Soundings from the Central Rae Domain of the Churchill Province, Nunavut; Geological Survey of Canada, Open File 7323, 34 p. doi:10.4095/292237

Spratt, J. E., Skulski, T., Craven, J.A., Jones, A.G., Snyder, D.B., and Kiyan, D., 2014. Magnetotelluric investigations of the lithosphere beneath the central Rae craton, mainland Nunavut, Canada; Journal of Geophysical Research: Solid Earth, 119, 2415–2439.

Steenkamp, H.M., Wodicka, N., Lawley, C.J.M., Peterson, T.D., and Guilmette, C., 2015. Overview of bedrock mapping and results from portable X-ray fluorescence spectrometry in the eastern part of the Tehery Lake–Wager Bay area, western Hudson Bay, Nunavut; in Summary of Activities 2015, Canada-Nunavut Geoscience Office, p. 121–134.

Steenkamp, H.M., Wodicka, N., Weller, O.M., and Kendrick, J., 2016. Overview of bedrock mapping in the northern and western parts of the Tehery Lake–Wager Bay area, western Hudson Bay, Nunavut; in Summary of Activities 2016, Canada-Nunavut Geoscience Office, p. 27–39.

Stern, R.A., Card, C.D., Pana, D., and Rayner, N., 2003. SHRIMP U-Pb ages of granitoid basement rocks of the southwestern part of the Athabasca Basin, Saskatchewan and Alberta; Radiogenic Age and Isotopic Studies: Report 16; Geological Survey of Canada, Current Research 2003-F3, 20 p.

Tella, S., Paul, D., Berman, R.G., Davis, W.J., Peterson, T.D., Pehrsson, S.J. and Kerswill, J.A. 2007. Bedrock geology compilation and regional synthesis of parts of Hearne and Rae domains, western Churchill Province, Nunavut – Manitoba. Geological Survey of Canada, Open File 5441, 3 sheets; 1 CD-ROM, https://doi.org/10.4095/224573

Therriault, I., Steenkamp, H.M. and Larson, K.P., 2017. New mapping and initial structural characterization of the Wager shear zone, north- western Hudson Bay, Nunavut; Summary of Activities 2017, Canada-Nunavut Geoscience Office, 1–12.

Thiessen, E.J., Gibson, H.D., Regis, D., and Pehrsson, S.J., 2018. Deformation and extensional exhumation of 1.9 Ga high-pressure granulites along the Wholdaia Lake shear zone, south Rae craton, Northwest Territories, Canada. Lithosphere, 10, 641-661.

Thiessen, E.J., Gibson, H.D., Regis, D., and Pehrsson, S.J., Ashley, K.T. and Smit, M.A. 2020. The distinct metamorphic stages and structural styles of the 1.94–1.86 Ga Snowbird Orogen, Northwest Territories, Canada. Journal of Metamorphic Geology, https://doi.org/10.1111/jmg.12556

Thomas, M.D., 2012. Shallow crustal structure in the Meadowbank River – Tehek Lake area: insights from gravity and magnetic modelling; Geological Survey of Canada, Open File 7308, 42 p.
Thompson, P.H., 1989. An empirical model for metamorphic evolution of the Archaean Slave Province and Adjacent Thelon Tectonic Zone, north-western Canadian Shield. in Evolution of Metamorphic Belts; Ed. Daly, J.S., Cliff, R.A., Yardley, B.W.D.; Geological Society, Special Publication 43, 245-263, https://doi.org/10.1144/gsl.sp.1989.043.01.17

Tschirhart, V., 2014. Geophysical and geological integration and interpretation of the northeast Thelon Basin, Nunavut. Ph.D. thesis, McMaster University.

Tschirhart, V., Morris, W.A. and Oneschuk, D., 2011a. Geophysical series, geophysical compilation project, Thelon Basin, Nunavut, NTS 66A, B, and parts of 65N, O, P, 66C, F, G and H. Geological Survey of Canada, Open File 6944, 1 sheet, doi:10.4095/288806.

Tschirhart, V., Morris, W.A., Ugalde, H., and Jefferson, C.W., 2011b. Preliminary 3D geophysical modelling of the Aberdeen sub-basin, northeast Thelon Basin region, Nunavut; Geological Survey of Canada, Current Research 2011-4, 12 p. doi: 10.4095/287165.

Tschirhart, P.A., Morris, W.A., and Jefferson, C.W., 2013a. Geophysical modeling of the Neoarchean Woodburn Lake and Paleoproterozoic Ketyet River groups, and plutonic rocks in central Schultz Lake map area, Nunavut; Geological Survey of Canada, Current Research 2013-2; 19 p. doi:10.4095/292116.

Tschirhart, V., Morris, W.A., Jefferson, C.W., 2013b. Framework geophysical modelling of granitoid vs. supracrustal basement to the northeast Thelon Basin around the Kiggavik uranium camp, Nunavut; Canadian Journal of Earth Sciences, 50, 667-677. doi.org/10.1139/cjes-2012-0149.

Tschirhart, V., Morris, W.A., Jefferson, C.W., 2013c. Faults affecting northeast Thelon Basin: improved basement constraints from source edge processing of aeromagnetic data; in Potter, E., Quirt, D., and Jefferson, C.W. (editors); Uranium in Canada: Geological Environments and Exploration Developments; Special Issue of Exploration and Mining Geology (CIM), 21, 105-113.

Tschirhart, V., Morris, W.A., Jefferson, C.W., Keating, P., White, J.C. and Calhoun, L., 2013d. 3D geophysical inversions of the north-east Amer Belt and their relationship to the geologic structure. Geophysical Prospecting, 61, 547-560. doi: 10.1111/j.1365-2478.2012.01098.x

Tschirhart, V., Morris, W.A. and Jefferson, C.W., 2014. Unconformity surface architecture of the northeast Thelon Basin, Nunavut, derived from integration of magnetic source depth estimates; Interpretation, 2, SJ263-SJ278. http://dx.doi.org/10.1190/INT-2014-0001.1.

Tschirhart, V., Percival, J.A., and Jefferson, C.W., 2015. Geophysical models of the Montresor metasedimentary belt and its environs, central Nunavut, Canada; Canadian Journal of Earth Sciences, 52, 833-845.

Tschirhart, V. and Pehrsson, S., 2016. New insights from geophysical data on the regional structure and geometry of the southwest Thelon Basin and its basement, Northwest Territories, Canada; Geophysics, 81, B167-B178.

Tschirhart, V.L., Wodicka, N. and Steenkamp, H., 2016. Shallow crustal structure of the Tehery Lake–Wager Bay area, western Hudson Bay, Nunavut, from potential-field datasets. in Summary of Activities 2016, Canada-Nunavut Geoscience Office, p. 41–50.

Tschirhart, V., Jefferson, C.W. and Morris, W.A., 2017. Basement geology beneath the northeast Thelon Basin, Nunavut: Insights from integrating new gravity, magnetic and geological data. Geophysical Prospecting, 65, 617–636. doi: 10.1111/1365-2478.12430.

Tschirhart, V., Craven, J., Potter, E., Powell, J., Pehrsson, S. and McEwan, B., 2019. Preliminary modelling of MT data in the Patterson Lake corridor, Saskatchewan, Canada; 16th Biennial SAGA Conference & Exhibition, extended abstracts, 3 p.

Tschirhart, V., Pehrsson, S., Card, C., Potter, E., Powell, J. and Pana, D., 2020. Interpretation of buried basement in the southwestern Athabasca Basin, Canada, from integrated geophysical and geological datasets; Geochemistry: Exploration, Environment, Analysis, 21(1).

Van Breemen, O., Peterson, T.D., and Sandeman, H.A., 2005. U–Pb zircon geochronology and Nd isotope geochemistry of Proterozoic granitoids in the western Churchill Province: intrusive age pattern and Archean source domains; Canadian Journal of Earth Sciences, 42, 339–377.

Walcott, R.I., Boyd, J.B., 1971. The gravity field of northern Alberta, and part of the Northwest Territories and Saskatchewan, with maps. Earth Physics Branch, Gravity Map Series No. 103-111, Ottawa, p. 13

Whalen, J.B., Berman, R.G., Davis, W.J., Sanborn-Barrie, M., and Nadeau, L., 2018. Bedrock geochemistry of the Thelon tectonic zone, Nunavut; Geological Survey of Canada, Open File 8234, 1 zip file. https://doi.org/10.4095/306385

Wheeler, J O; Hoffman, P F; Card, K D; Davidson, A; Sanford, B V; Okulitch, A V; Roest, W R. 1996. Geological map of Canada / Carte géologique du Canada; Geological Survey of Canada, "A" Series Map 1860A.

Wodicka, N., St-Onge, M.R., Corrigan, D., Scvott, D.J., and Whalen, J.B., 2014. Did a proto-ocean basin form along the southeastern Rae cratonic margin? Evidence from U-Pb geochronology, geochemistry (Sm-Nd and whole-rock), and stratigraphy of the Paleoproterozoic Piling Group, northern Canada. Bulletin of the Geological Society of America, 126, 1625-1653. doi: 10.1130/B31028.1

Wodicka, N., Steenkamp, H.M., Weller, O.M., Kendrick, J., Tschirhart, V.L., Peterson, T.D., and Girard, É., 2016. Report of 2016 Activities for the Bedrock Geology and Economic Potential of the Tehery- Wager Area: GEM 2 Rae Project; Geological Survey of Canada, Open File 8149, 21 p. doi:10.4095/299392

Wodicka, N., Steenkamp, H.M., Peterson, T.D., McMartin, I., Day, S.J.A., and Tschirhart, V.L., 2017. Report of 2017 activities for the geology and economic potential of the Tehery-Wager area, Nunavut: GEM-2 Rae Project; Geological Survey of Canada, Open File 8318, 20 p. https://doi.org/10.4095/305979